Recent Progress in Acoustic Metamaterials and Active Piezoelectric Acoustic Metamaterials – A Review

Guosheng Ji*, John Huber**

Department of Engineering Science, University of Oxford, Parks Road, Oxford, OX1 3PJ, UK

ARTICLE INFO

Keywords:
active
passive
piezoelectric
acoustic metamaterial
acoustic metasurface

ABSTRACT

Acoustic metamaterials, structured to produce anomalous reflection and refraction indices that are not found in conventional materials, are gaining prominence in engineering applications. These artificial structures have enabled novel functionalities, such as negative effective properties, extraordinary wave manipulation, enhanced sound absorption and insulation, cloaking, acoustic wave focusing, and efficient energy harvesting. To evaluate the research progress in the field of acoustic metamaterials, we take a novel viewpoint, tracing the development from passive acoustic metamaterials to active piezoelectric acoustic metamaterials. The article summarizes recent research progress in acoustic metamaterials, with the first part describing passive acoustic metamaterials and the second part moving on to active piezoelectric acoustic metamaterials and metasurfaces. The topics covered include their general definition, mechanisms, classification, structure, and potential applications. Finally, we survey the current technical challenges from a practical engineering standpoint and discuss the future outlook in this field.

1. Introduction

Walser defined metamaterials by stating that metamaterials are so-named to recognize and emphasize their purpose to improve material properties beyond conventional composites' limitations [1]. In practice, metamaterials are usually artificial materials composed of periodical sub-wavelength structures with properties and functionalities that are not normally found in nature [2].

The earliest research work in developing metamaterials dealt with electromagnetism. In general, fundamental parameters to define electromagnetic field behaviours in a medium are the relative dielectric permittivity ϵ, relative magnetic permeability μ, and the index of refraction $n = \sqrt{\epsilon \cdot \mu}$, which normally are positive numbers greater than or equal to unity. Veselago indicated that a medium with simultaneously negative ϵ and μ might result in negative refraction in the electromagnetic field in the middle of the nineteenth century [3]. However, the way to create materials with negative indices of refraction was not known until about thirty years later, when Pendry created the wire medium structure [4] and the split ring structure [5] to generate the negative permittivity ϵ and negative permeability μ, respectively. Inspired by Pendry's work, Smith *et al.* proposed the so-called double negative metamaterials with high engineering feasibility [6] and observed the anomalous negative refraction phenomenon in the laboratory for the first time [7]. The concept of electromagnetic metamaterials introduced rapid development in optics [8–10] and the related fields of acoustics [11, 12], mechanical vibration [13, 14], and even heat conduction [15–17], where waves share similar physical features.

Acoustic metamaterials (AMs) are artificial materials with anomalous effective properties that can manipulate acoustic waves, and have been studied over the last twenty years. A summary of research milestones in the area of metamaterials and specifically AMs is given in Table 1. Passive AMs generally cannot provide external energy input into acoustic waves. The initial passive sub-wavelength meta-atom was created to demonstrate high sound transmission loss [11], and passive AMs were subsequently classified into sub-wavelength meta-atoms and periodical acoustic metasurfaces in the form of space coiling structures, Helmholtz resonators, membrane resonators, and porous metamaterials.

In recent years, active elements started to be incorporated into AMs. Examples include piezo-shunting, structural deformations that alter properties, controllable temperature, pressure, electric field and magnetic field effects. Active

*Corresponding author
**Principal corresponding author
guosheng.ji@eng.ox.ac.uk (G. Ji); john.huber@eng.ox.ac.uk (J. Huber)
ORCID(s):

AMs offer the opportunity of anomalous effective material properties at adjustable frequencies; specifically, active piezoelectric AMs have great potential as AMs combined with the opportunity for solid-state electronic control. Potential applications that have been identified include anomalous wave manipulation, extraordinary sound absorption and insulation, acoustic focusing, and cloaking in both two and three-dimensional spaces, going far beyond conventional materials.

Table 1
Milestones in metamaterials, AMs and active piezoelectric AMs.

Year	Authors	Research milestones
1967	Veselago [3]	Proposed a basic theory of abnormal materials with simultaneously negative dielectric permittivity and magnetic permeability.
1996	Pendry [4]	Proposed theoretical guides to design materials with negative permittivity ("wire medium" structure).
1999	Pendry [5]	Proposed theoretical guides to design materials with negative permeability ("split ring" structure).
2000	Liu [11]	Designed and tested AMs with negative mass density.
2001	Shelby [7]	Experimentally verified the negative refraction phenomena.
2004	Movchan [18]	Designed and tested membrane-type AMs with negative mass density.
2004	Li [19]	Theoretically proposed double negative AMs with simultaneously negative mass density and bulk modulus.
2006	Fang [20]	Proposed and experimentally achieved Helmholtz resonator chains with negative bulk modulus.
2009	Baz [21]	Proposed active piezoelectric AMs with negative density.
2010	Lee [22]	Experimentally proved the existence of double negative AMs.
2010	Akl [23]	Proposed active piezoelectric AMs with negative bulk modulus.
2010	Akl [24]	Proposed active piezoelectric AMs with double negative properties.
2011	Yu [10]	Proposed the generalized Snell's law and experimentally proved the existence of anomalous reflected and refracted phenomena in optics.
2012	Aieta [25]	Proposed a more general Snell's law for flat and spherical interfaces.
2013	Li [12]	Numerically proposed designs of acoustic metasurface based on the generalized Snell's law.
2014	Li [26]	Experimentally proved the existence of anomalous reflection phenomena in scattered sound pressure fields.
2015	Popa [27]	Designed active acoustic metasurface to achieve various anomalous phenomena without changing their physical structure.
2019	Ju [28]	Introduced the geometry curvature effect into AM structures.
2020	Li [29]	Designed curved AMs for reflected wave-front modulation in three-dimensional space.

The development of AMs has been extensively surveyed from analytical [30–33] and engineering [34–37] perspectives, from the early discovery of negative characteristics to their diverse functionalities and implications. Several new research directions and early results have been addressed extensively, including wave manipulation in fluids, elastic and mechanical materials, graphene-inspired AMs, non-reciprocal AMs, unidirectional sound insulators, soft AMs, and actively controlled AMs, etc [30–38]. These reviews mainly emphasize the fundamental concepts and applications of AMs, but the research milestones of metamaterials and AMs are not clearly outlined. Consequently, comprehensive surveys of the most promising applications in airborne sound absorption, insulation, and energy harvesting are still necessary.

These general evaluations have highlighted a promising future and growing efforts to investigate active AMs, which may be able to overcome the challenges of passive AMs and improve their effectiveness in relevant applications [30–38]. Research progress on active and tunable AMs has been reviewed by other researchers, with working principles ranging from mechanical factors such as shape deformation, controllable pressures, and fluid-structure interactions to electronic factors such as electric fields, magnetic fields, and piezo-shunting methods being considered [39–41]. Among them, active piezoelectric AMs have attracted growing research interest, giving rise to a need to understand the relationship between passive AMs and active piezoelectric AMs and to identify potential research directions for

future study in the area of piezoelectric AMs. Therefore, there is a need for a comprehensive study to include a clear picture of the current research and engineering challenges associated with passive AMs and active piezoelectric AMs. As a consequence, a reassessment of the research frontier relating passive AMs to active piezoelectric AMs is needed, given their tremendous potential and ability to be controlled electronically. The present review aims to provide this link and explore distinctions between passive AMs and active piezoelectric AMs in detail. It thus provides a concise overview of AMs, research insights, and associated terms and outlines of the development from passive AMs to active piezoelectric AMs.

In the present work, the categorization of AMs is based on their fundamental material mechanics and physical mechanisms. The comprehensive assessment focuses on advances in AMs, including design concepts, materials, manufacturing techniques, structural optimization, various enhanced acoustic properties, and applications. We describe practical solutions to many problems while simultaneously presenting a slew of unresolved ones. Additionally, we systematically review rapidly emerging porous AMs and active piezoelectric AMs, presenting the most significant advances in fundamental design concepts and structural optimization, in conjunction with practical manufacturing, to achieve a variety of extraordinary acoustic properties. Finally, the review identifies applications and potential challenges in this attractive field of research.

The review is structured as follows: we firstly summarize the definition, mechanism, general arrangement, and classifications of passive AMs. The main objective of this section is to provide essential background and introduce the terms necessary for describing subsequent research development. Then, the functional mechanisms of active AMs with piezoelectric materials as active elements are reviewed, along with their potential applications in active acoustic waveguides, wave manipulators, sound absorbers, insulators, and energy harvesters. Finally, conclusions and a future outlook in the area of passive AMs and active piezoelectric AMs are given.

2. Fundamentals

2.1. Concept of acoustic metamaterials

The fundamental equation governing the acoustic wave propagation inside homogeneous media in the absence of internal sound sources is [42]:

$$\nabla^2 p - \frac{\rho}{\kappa}\frac{\partial^2 p}{\partial t^2} = 0, \tag{1}$$

where p is the sound pressure, t is time, ρ and κ are the medium's mass density and bulk modulus, respectively. The specific acoustic impedance, Z, which controls wave reflection and refraction amplitudes at interfaces, is defined as the ratio of pressure to fluid velocity: $Z = p/v = \sqrt{\rho\kappa}$. In natural media, ρ and κ normally take positive values that are inherent to their material composition and microstructures. However, AMs, constructed with sub-wavelength resonant meta-atoms, can enhance sound-matter interactions resulting in macroscopic behaviour like a continuous material with unconventional effective properties. Broadly defined, AMs are assemblies of sub-wavelength meta-atoms with unusual homogenized acoustic properties and functionalities.

2.2. Mechanism of acoustic metamaterials

The mechanism of resonant acoustic meta-atoms with deep sub-wavelength sizes relies on oscillators that generate out-of-phase responses to modify wave propagation [11, 20, 43, 43–45]. Fano interference can result in a negative effective mass density and an imaginary wave vector [11, 43, 43–46]. Another strategy is to design sub-wavelength AMs with resonance-induced negative bulk modulus [47, 48], such as Helmholtz resonator chains [20]. Furthermore, by overlapping the frequency ranges of negative effective mass density and negative bulk modulus, double-negative AMs can be formed [22, 49–51] that demonstrate unusual acoustic properties.

Acoustic metasurfaces work as wavefront shaping devices with deep sub-wavelength thickness. Their unusual acoustic properties and functionalities are usually induced by sub-wavelength space coiling channels [12, 52, 53] or highly resonant inclusions [54–58]. The deep sub-wavelength structures enable acoustic wave manipulation through spatial phase gradient shifts, which can be achieved by space coiling elements [12, 52, 53], Helmholtz resonators [54–58], resonant membranes and plates [59–61], or porous materials [62–65]. For instance, space coiling structures can slow down the acoustic wave speed inside AMs to achieve large refractive indices and desired spatial phase gradients, broadening their operating bandwidth and avoiding resonance-induced energy dissipation [12, 52, 53]. As a result, acoustic metasurfaces have the ability to control the phase gradients and amplitudes of impinging acoustic waves.

AMs provide a way to manipulate the effective constitutive parameters of natural media at particular frequencies, offering a wide range of values, including negative values. This enables AMs to demonstrate a variety of anomalous phenomena.

2.3. Mass law

The transmission loss of airborne acoustic waves through an assembly normally obeys a mass law in a certain frequency and density range. This can be expressed as [66]:

$$\mathrm{TL}\,(\theta) = 10\log\left[1 + \left(\frac{\omega \mathrm{m_s}\cos\theta}{2\rho_0 \mathrm{c}}\right)^2\right], \tag{2}$$

where TL(θ) is the transmission loss of an assembly at an incidence angle θ, m_s is the mass per unit area, and ω is the acoustic wave angular frequency. ρ_0 and c are the air density and sound speed in air, respectively. The most important physical property to determine the value of the transmission loss through an assembly at a specific frequency, mass per unit area m_s, is a product of the material density and its thickness. Equation 2 predicts that the transmission loss of an assembly at a certain frequency increases by 6 dB once the mass per unit area is doubled. Mass per unit area can be increased by increasing thickness or by selecting a more dense material. AMs provide a way to break the mass law and thereby achieve a greater transmission loss than other materials without a high mass requirement.

3. Passive acoustic metamaterials

Passive AMs do not provide energy to the AM system that is excited by an incident acoustic wave; anomalous phenomena are realized without external energy input, and the frequency response is fixed by the structural design. Currently, passive AMs can be divided into several groups according to the artificial structure that achieves the anomalous effects: sub-wavelength meta-atoms, periodic acoustic metasurfaces with space coiling structures, Helmholtz resonators, membrane and plate resonators, and porous materials.

3.1. Sub-wavelength meta-atoms

Sub-wavelength meta-atoms are components of artificial materials with unit cells periodically or randomly hosted in a specially designed matrix. The resulting meta-atom can affect impinging acoustic waves as a homogeneous material with unusual physical properties. The sub-wavelength meta-atoms can be divided into three main types determined by their unusual effective mass density and bulk modulus, as shown in Figure 1.

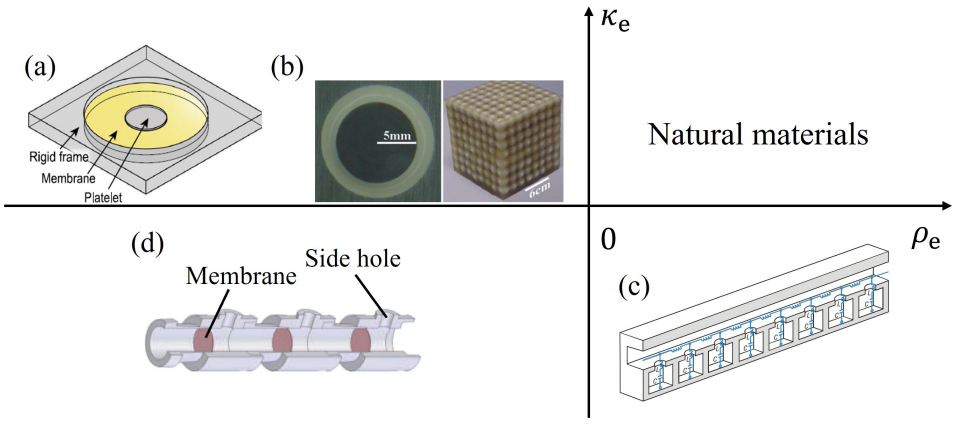

Figure 1: Sub-wavelength resonating meta-atoms. (a) Membrane-type meta-atoms. Reprinted by permission from [43], Copyright 2014 Springer Nature. (b) Locally resonant sonic crystal. From [11], Reprinted with permission from AAAS. (c) Helmholtz resonator chains. Reprinted by permission from [20], Copyright 2006 Springer Nature. (d) Double negative meta-atoms. Reprinted figure with permission from [22], Copyright 2010 by the American Physical Society.

3.1.1. Meta-atoms with negative effective mass density

A spring-mass model is generally used to describe the mechanism of meta-atoms with negative effective mass density, which consists of a spring structure with a low bulk modulus and density combined with a mass structure with a high bulk modulus and density. The relative motion of the mass is given by [67, 68]:

$$F = m_e \ddot{x}, \tag{3}$$

where F and m_e are the external harmonic excitation force and the effective system mass, respectively. $\ddot{x}$ is the relative acceleration of the mass structure. The effective system mass m_e is then determined by:

$$m_e = m_1 + \frac{\kappa}{\omega_0^2 - \omega^2}, \tag{4}$$

where m_1 is the mass of the mass structure, $\kappa = \omega_0^2 m_2$ is the bulk modulus of the spring structure with m_2 as the mass of the spring structure , and ω_0 and ω are the resonant angular frequency of the spring structure and the angular frequency of the external force, respectively. Accordingly, the effective mass density can be defined by $\rho_e = m_e/V_e$, where V_e is the effective volume of the system. The effective system mass m_e could become negative when the driving frequency ω approaches ω_0 from above, which will result in strong energy dissipation [68].

For a typical membrane-type AM with a mass attached, as shown in Figure 1(a), the vibrational governing equation under planar incident waves becomes [69]:

$$\rho_1 h_1 \frac{\partial^2 W_1(x,y,t)}{\partial t^2} - T\nabla^2 W_1(x,y,t) = p_1 - p_2 + \Sigma_{i=1}^{I} Q_i(t)\delta(x - x_i)\delta(y - y_i), \tag{5}$$

where $W_1(x, y, t)$ is the out-of-plane displacement of the membrane in the z direction in the Cartesian coordinate system (x, y, z), $p_1 - p_2$ is the sound pressure difference across the membrane, δ is the Dirac delta function, T is the uniform tension per unit length, t is time, ρ_1 and h_1 are the density and thickness of the membrane, respectively. $\Sigma_{i=1}^{I} Q_i(t)\delta(x - x_i)\delta(y - y_i)$ is the summation of point forces at collocation points on the interface between membrane and mass structures.

In laboratory tests, Liu *et al.* proposed a locally resonant meta-atom made of a solid ball core material as the mass structure and soft silicone rubber as the spring structure, as shown in Figure 1(b). The crystal lattice size was two orders of magnitude smaller than the corresponding acoustic wavelength. At the operating frequency, complete sound attenuation and a negative effective mass density were observed [11]. The appearance of locally resonant meta-atoms breaks the so-called mass law in which the sound transmission loss through a wall is proportional to the thickness and density of the wall as well as the angular frequency of incident waves. Yang *et al.* [70] proposed the first membrane-type AM with a mass structure attached at the center, which could tune the vibrational eigenfrequency and lead to various transmission behaviours. Near-total sound reflection could be achieved at the minimum transmission coefficient in Figure 2(a), where the in-plane averaged normal vibration amplitude was minimum and the effective dynamic mass of the resonator was negative, as shown in Figure 2(b).

Various spring-mass types of meta-atoms with negative effective mass density were further proposed, such as aluminium blocks [71], split-ring resonator structures [18], plate-type meta-atoms [72, 73], membranes and shell-type meta-atoms [43–45, 70, 74, 75]. Meta-atoms scale down sonic crystals to the deep sub-wavelength size, where Fano interference that occurs between a continuum state and a sharply localized state plays a crucial role [46]. However, constrained by structural characteristics, the crystal only works efficiently over a very narrow frequency range that may be far from the requirements of practical applications. Besides, meta-atoms with negative effective mass density are always associated with the displacement of the mass center, which unavoidably introduces energy dissipation into the system.

3.1.2. Meta-atoms with negative effective bulk modulus

Meta-atoms in sub-wavelength sizes can also be realized by bringing in structures with resonance-induced negative bulk modulus, such as Helmholtz resonator chains. Helmholtz resonators, consisting of a simple chamber with a narrow neck, can convert acoustic energy into heat through vibration resistance. This process is governed by the spring-mass model, where the small fluid element in the narrow neck works as an effective oscillating mass, and the fluid contained in the chamber body works as an effective spring. If the size of the Helmholtz resonators is much smaller than the

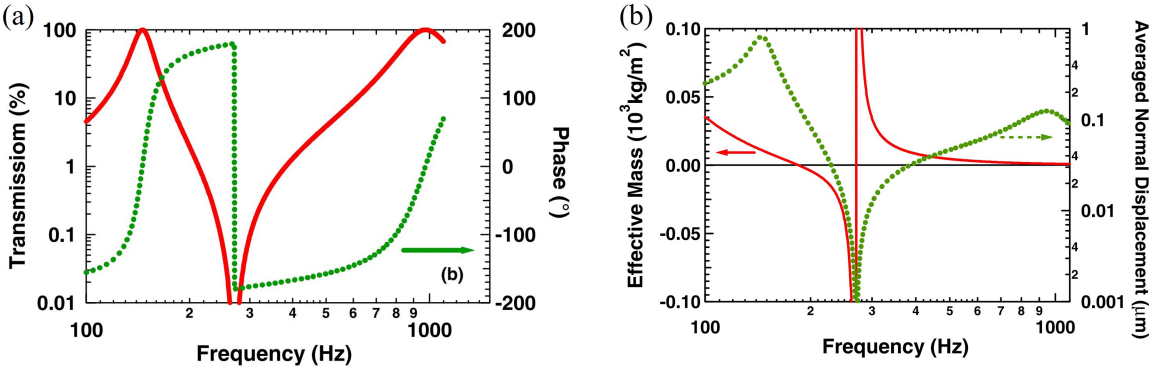

Figure 2: (a) Transmission amplitude (red curve) and phase (green curve) of the membrane resonator, and transmission amplitude predicted by the mass density law (blue line). (b) Effective dynamic mass of the resonator (red curve) and in-plane averaged normal vibration amplitude (green curve). Reprinted figure with permission from [70], Copyright 2008 by the American Physical Society.

incident acoustic wavelength, under adiabatic and harmonic sound pressure conditions, its resonant frequency is given by [76]

$$f = \frac{c}{2\pi}\sqrt{\frac{S_n}{Vl}}, \tag{6}$$

where l is the effective length of the neck, V is the chamber's volume, c is the sound speed in the fluid, and S_n is the cross-sectional area of the neck. Various types of acoustic resonators, such as perforated panels and micro-perforated panels, share a similar physical mechanism in terms of the compression-extensional motion inside the cavity of resonators by dividing the initial neck of a Helmholtz resonator into numerous smaller ones [77–79]. As a result, a pressure fluctuation in the channel serves as a source, compressing and extending the liquid contained inside the cavity, which results in a frequency-dependent effective bulk modulus.

Helmholtz resonator chains in Figure 1(c) can be used to produce a negative effective bulk modulus. In these structures, acoustic inductance and capacitance can be controlled by adjusting the neck and cavity of the resonators, respectively. The sound transmission of the one-dimensional AM was measured underwater as a function of frequency. Its effective bulk modulus κ_e is defined as [20]:

$$\kappa_e^{-1}(\omega) = \kappa_0^{-1}\left(1 - \frac{G\omega_0^2}{\omega^2 - \omega_0^2 + iD\omega}\right), \tag{7}$$

where G is a geometrical factor, ω_0 is the resonant angular frequency, i is the imaginary number, and D is the dissipation loss in the resonating elements. A region of negative effective dynamic bulk modulus was observed near the resonance frequency in experiments with the group velocity anti-parallel to the phase velocity [20], indicating potential applications in negative refraction and super-lenses.

Inspire by this study, a variety of meta-atoms with negative effective bulk modulus, such as quasi-two-dimensional Helmholtz resonators [47, 48, 48], foams [80], as well as topology optimization for sub-wavelength meta-atom designs [81], were explored. However, Helmholtz resonator chains do not work efficiently over a wide frequency range for two or three-dimensional structures. This is primarily because two or three dimensional Helmholtz resonator chains are much more complex in internal structure, with the consequence that negative bulk modulus values can only be obtained across a narrow frequency range.

3.1.3. Meta-atoms with double negative effective property

In general, the resonant mode of meta-atoms can be used as an indicator of their effective properties. A monopole source that radiates sound equally in all directions contributes to a compressive-extensional response and a dispersive bulk modulus. In contrast, a dipole source can be realized by placing two monopoles of equal strength but opposite

polarity together, spaced by a distance shorter than the acoustic wavelength. This leads to a displacement of the central mass and a dispersive mass density. By overlapping the resonant frequency spectra, the effective mass density and bulk modulus of acoustic meta-atoms can be simultaneously dispersive and negative over the same frequency range. Numerous analytical models of meta-atoms have been investigated that exhibit both negative mass density ρ and bulk modulus κ, such as a rubber sphere structure model [19], a zinc blende structure model [82], a one-dimensional array consisting of shunted Helmholtz resonators [83], and a rubber-coated water cylinder embedded in a foam host [84].

Lee *et al.* [22] demonstrated the existence of acoustic meta-atoms with double negative effective properties in an experimental test, which consists of a periodic array of inter-spaced membranes and side holes, as shown in Figure 1(d). In this model, the effective density ρ_e of a tube with an array of thin tight membranes is a function of frequency ω:

$$\rho_e = \rho'(1 - \omega_c^2/\omega^2), \tag{8}$$

where ρ' is the average density of the fluid between membranes, and ω_c is the cut-off frequency of the array of membranes. The bulk modulus κ_e of a tube with an array of side holes is:

$$\kappa_e = \kappa(1 - \omega_s^2/\omega^2)^{-1}, \tag{9}$$

where ω_s is its cut-off frequency, and κ is the bulk modulus of air. The transmission, effective density, and phase velocity of meta-atoms were measured in the laboratory, and negative density and bulk modulus were simultaneously observed for the first time [22].

The anomalous phenomena generated by acoustic meta-atoms with double negative effective properties and their potential applications were widely studied analytically, numerically and in laboratory tests. For example, negative refraction of acoustic waves [85] and elastic waves [86] could be generated by novel chiral microstructures over a relatively broad frequency range. Double negativities were also observed in coupled membrane structures [87]. Besides, the transmission and reflection behaviours of various acoustic meta-atoms were also investigated, such as three-dimensional flute-model structures [88], unitary meta-molecule structures [89], labyrinthine resonating structures [49, 50], a two-dimensional comb-like interlayer structure [51], and a three-dimensional hollow steel tube structure [90].

It should be pointed out that the complicated structures of meta-atoms and their resonances mainly determine the anomalous properties of all these sub-wavelength resonating structures. As a consequence, acoustic meta-atoms with negative effective properties operate only within a very limited frequency range. For sound insulation and absorption applications, meta-atoms are of limited use because a wide frequency range corresponding to human hearing (∼20 Hz to ∼20 kHz) must be suppressed.

3.2. Periodic acoustic metasurfaces

Locally resonant acoustic meta-atoms provide a way to generate unusual effective properties and anomalous phenomena, but challenges of operating bandwidth still exist due to their resonant nature. Periodic acoustic metasurfaces have been proposed to avoid energy dissipation and broaden operating bandwidth. A periodic acoustic metasurface is a functional surface containing sub-wavelength structures, and it is capable of generating local phase shifts. The primary function of the acoustic metasurface lies in its unique ability to manipulate acoustic wave propagation in the scattered sound pressure field.

The wave manipulation function of the acoustic metasurface can be well predicted using the generalized Snell's law [10, 91]:

$$n_t \sin\theta_t - n_i \sin\theta_i = \frac{\lambda_0}{2\pi}\frac{d\Phi}{dx}, \tag{10}$$

where Φ is the local phase shift at the position x on the metasurface. n_t and n_i are the refraction indices in the refracted medium and the incident medium, respectively. θ_t and θ_i are the angles of refraction and incidence, respectively, and λ_0 is the free-space wavelength.

An analogy between the generalized refraction and diffraction theory was proposed in a more general form considering the existence of extra refraction modes [92]. Governed by the generalized Snell's law, the reflected or refracted wave direction can be manipulated at will by adjusting the local phase shift gradients $d\Phi/dx$. For instance, by adopting a two-dimensional resonator array with spatially varying phase shifts, anomalous reflection and refraction phenomena was observed in light propagation for the first time [10], and then similar effects were expected in acoustic waves. The generalized Snell's law can be extended to an acoustic counterpart by creating periodic arrays of sub-wavelength units, such as coiled-up space structures, Helmholtz resonators, membranes, plates, and porous materials, to generate the desired phase shifts and then manipulate the acoustic waves.

3.2.1. Acoustic metasurface with space coiling structures

Through the use of sub-wavelength curled channels, a space coiling acoustic metasurface develops anomalous effective properties. The space coiling unit cells are able to slow down and control effective sound speeds inside AMs, which helps achieve large refractive indices and desired spatial phase gradients. This can broaden the operating bandwidth and avoid resonance-induced energy dissipation. For example, an ultra-thin planar acoustic metasurface, constructed with eight units of a space coiling structure (a typical unit given in Figure 3(a)), can generate discrete local phase shifts over a 2π span with steps of $\pi/4$ as shown in Figure 3(b) [12]. By proper selection of the phase shift profile and periodic length, anomalous wavefront phenomena, such as anomalous reflections, conversion from propagating waves into surface waves, and a planar aberration-free lens, were demonstrated in numerical simulations. Theoretical study and experimental validation came shortly afterwards, with the observation of anomalous refraction phenomena governed by the generalised Snell's law [26].

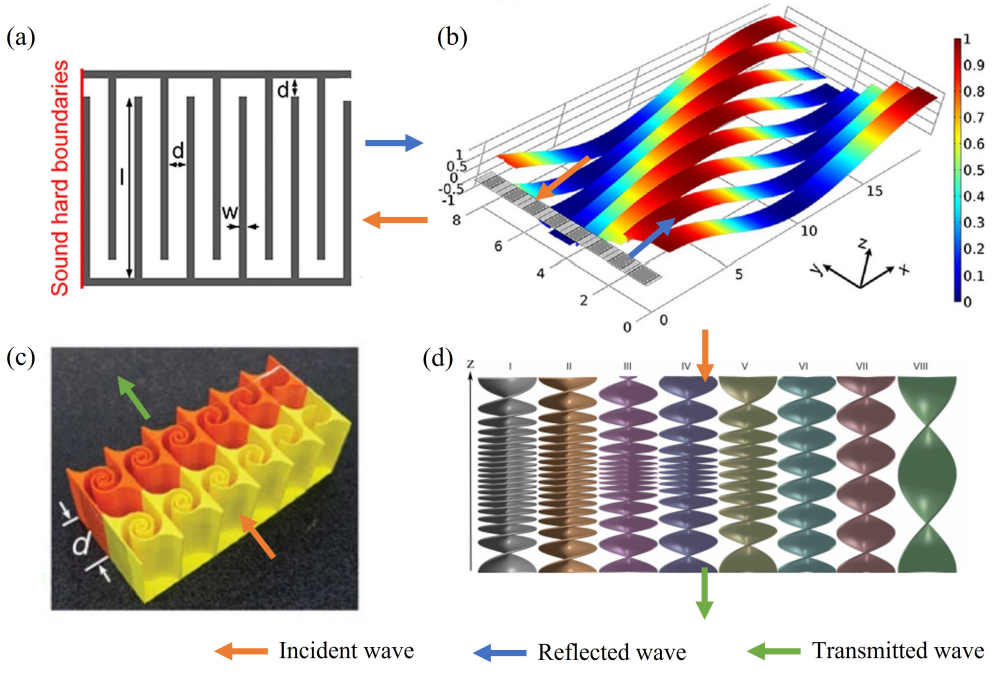

Figure 3: Space coiling structures. (a) Configuration of a typical unit. Reprinted by permission from [12], Copyright 2013 Springer Nature. (b) Phase shift profile of various units. Reprinted by permission from [12], Copyright 2013 Springer Nature. (c) Tapered labyrinthine structure. Reprinted by permission from [52], Copyright 2014 Springer Nature. (d) Space-coiled cylindrical structure. Reprinted by permission from [53], Copyright 2017 the American Physical Society.

The classical space-coiling structure was further developed into many geometries that demonstrate specific wave manipulation functions, such as coiling-slit units [96], tapered labyrinthine structures (Figure 3(c)) [52, 97], horn-like space-coiling structures [98], space-coiled cylindrical structures (Figure 3(d)) [53], tapered corrugated holes [95], rigid thin plates decorated with sub-wavelength slits [99], sandwich-like space-coiling structures [100], a helical channel with screw structure [101, 102], multi-coiled metasurface with labyrinthine channels and perforated plates [103], and so on.

Transmitted acoustic waves can also be manipulated by a space coiling acoustic metasurface with a sub-wavelength thickness [96]. Anomalous phenomena such as beam-steering (Figure 4(a)) and conversion of propagating waves to evanescent surface waves (Figure 4(b)) were observed using a tapered labyrinthine acoustic metasurface [52, 97]. Numerous studies have shown superior performance in space coiling acoustic metasurfaces for real-world applications, including simultaneous modulation of phase shifts and amplitudes of transmitted waves [98], manipulation of sound radiation patterns (Figure 4(c)) [93], one-way acoustic wave propagation (Figure 4(d)) [94], three-dimensional acoustic focusing (Figure 4(e)) [95], acoustic vortex generation (Figure 4(f)) [53], acoustic focusing with high transmission efficiency and ultra-broadband frequency range [99, 100], broadband high sound absorption [104], and cloaking [105].

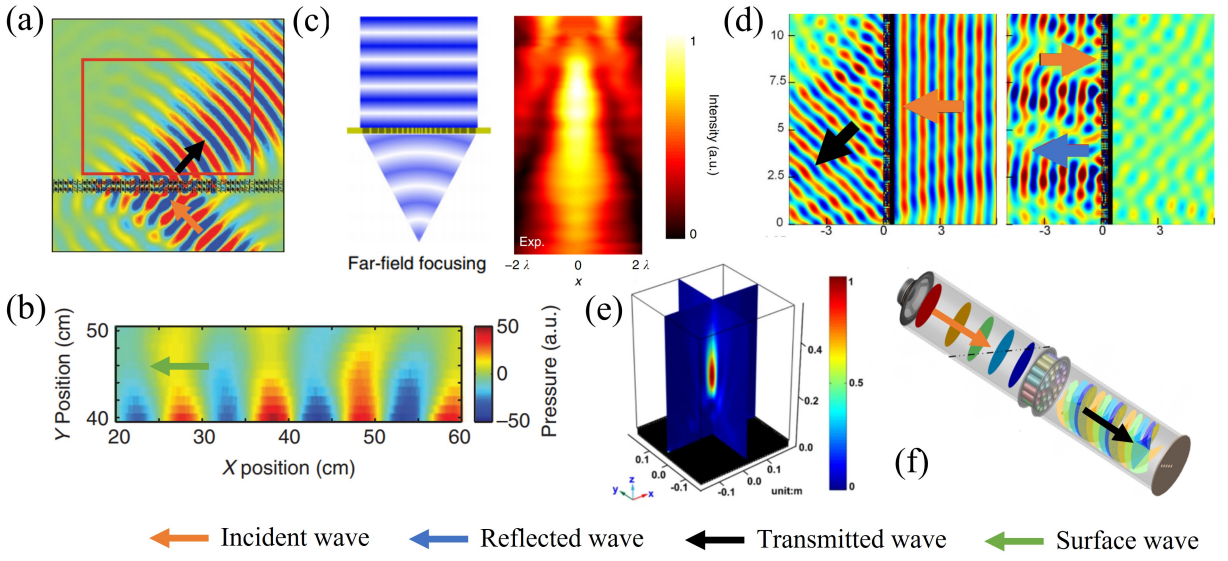

Figure 4: Applications of space coiling structures. (a) Negative refraction. Reprinted by permission from [52], Copyright 2014 Springer Nature. (b) Propagating-to-surface-wave conversion. Reprinted by permission from [52], Copyright 2014 Springer Nature. (c) Plane wave focusing. Reprinted by permission from [93], Copyright 2018 Springer Nature. (d) One-way acoustic metasurface. Reprinted by permission from [94], Copyright 2016 Springer Nature. (e) Three-dimensional acoustic focusing. Reprinted by permission from [95], Copyright 2019 Springer Nature. (f) Acoustic vortex generation. Reprinted by permission from [53], Copyright 2017 the American Physical Society.

Space coiling structures provide a new way to manipulate acoustic waves by steering spatial phase shift gradients. However, challenges still exist in terms of their complexity in structure and the impedance mismatch between metasurfaces and background media. Some of these challenges can be met by using alternative resonators, such as Helmholtz resonators. Another issue with this kind of acoustic metasurface is how to integrate it with other absorbent materials such as porous foams or soft materials to allow excellent sound absorption and insulation properties. Topology optimization for acoustic metasurfaces with space coiling structures has been established, assisting solution of the design problem [106]. Computer analysis enables systematic optimization of the shape and topology in order to enhance the acoustic performance under defined constraints. As a result, it is likely that topology optimization will increasingly play a role in the design of acoustic metasurfaces with space coiling structures.

3.2.2. Acoustic metasurface with Helmholtz resonators

Acoustic metasurfaces with Helmholtz resonators can generate a desired phase shift gradient through the tailoring of resonator structures. The resulting metasurface can have superior properties, such as broad bandwidth, high transmission coefficient, well-matched acoustic impedance, and ease of fabrication.

In order to manipulate reflected acoustic waves, an acoustic metasurface consisting of hollow sphere resonator arrays, as shown in Figure 5(a), can generate desired phase shifts in reflected waves, and this can be controlled by adjusting the neck lengths (Figure 5(b)). This enables the manipulation of incident acoustic waves into surface waves or reflected waves at any angle [54, 107]. An array with varying-depth Helmholtz resonators in Figure 5(d), which overcomes the narrow bandwidth limitations of a conventional metasurface by introducing chambers with linearly increased depth, possesses the functionality of both reflected wave manipulation and sound energy attenuation simultaneously over a broadband frequency range [56, 108]. In Figure 5(e), Helmholtz resonators with varying internal coiled path lengths [57] were created to realize beamforming functions by introducing reflected phase shifts that vary along an acoustic metasurface.

As for the manipulation of transmitted acoustic waves, acoustic metasurfaces made of metal units with four Helmholtz resonators and a single slit in Figure 5(c) and various cavity depths in Figure 5(f) enable wide effective

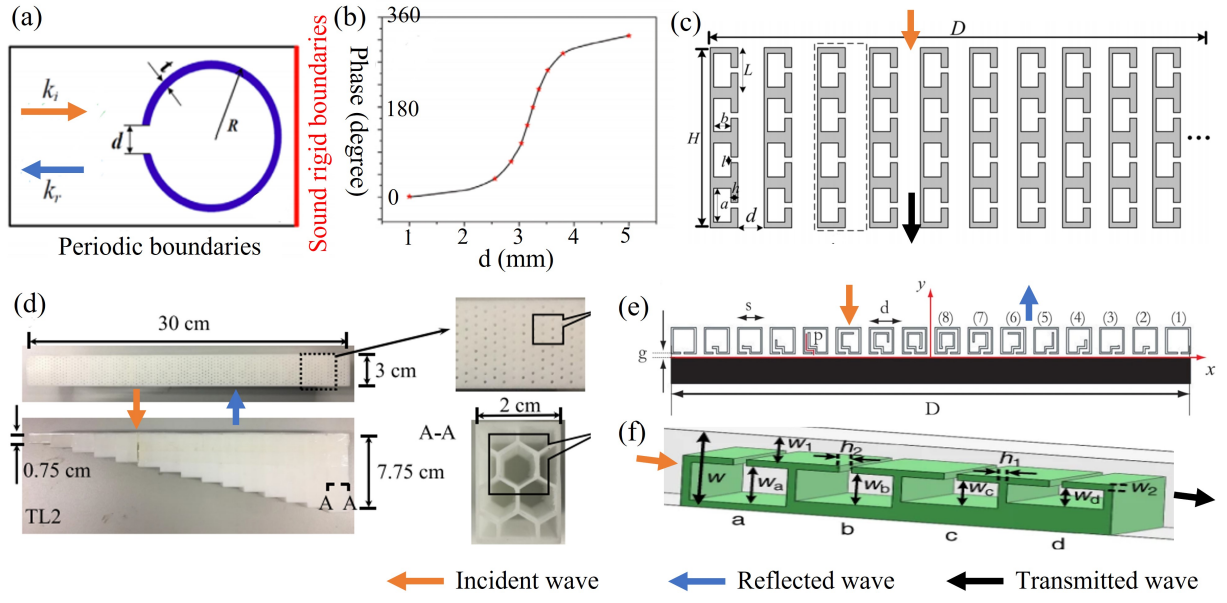

Figure 5: Helmholtz resonator type of acoustic metasurfaces. (a) Configuration of a Helmholtz resonator. Reprinted by permission from [54], Copyright 2015 IOP Publishing. (b) Phase shift profile for various neck lengths. Reprinted by permission from [54], Copyright 2015 IOP Publishing. (c) Complex acoustic metasurface with Helmholtz resonators and a single slit. Reprinted by permission from [55], Copyright 2017 Springer Nature. (d) Perforated panels with varying-depth chambers. Reprinted from [56], with the permission of AIP Publishing. (e) Helmholtz resonators with varying internal coiled path lengths. Reprinted by permission from [57], Copyright 2016 Springer Nature. (f) Helmholtz resonator with varying-depth chambers. Reprinted by permission from [58], Copyright 2018 Springer Nature.

bandwidth with excellent impedance matching and high transmission efficiency [55, 58, 109]. Analytical, numerical and experimental results indicate that several types of anomalous wavefront manipulations can be achieved using Helmholtz resonators, such as non-diffracting Bessel beam [55], cloaking [110, 111], propagating-to-surface wave conversion [54], bi-anisotropic wavefront transformation [112, 113], and cylindrical-to-plane wave conversion [55] in two and three-dimensional space [29].

Recent years have seen tremendous advances in manufacturing technology, with diverse additive manufacturing techniques reducing the structural size scale and fabrication cost of acoustic metasurfaces as well as improving fabrication precision, which enables the manufacture of a range of complex structures [54, 55, 110, 113]. The resulting freedom of structural design enables AMs with Helmholtz resonators to meet a wider variety of external requirements, and thus extends the range of applications. However, the principal drawback of this kind of acoustic metasurface remains, namely the difficulty in achieving practically useful effects over a wide frequency range.

3.2.3. Acoustic metasurface with membrane and plate resonators

Membrane and plate resonators achieve similar effects to Helmholtz resonators via a different mechanism. By adjusting the tension applied to the membrane [59] or the weight and shape of an attached mass, as shown in Figure 6(a), membrane-type resonators can generate desired phase shift gradients within one periodic length. For plate type resonators, the plate stiffness [114] plays a crucial role in manipulating the reflected phase shifts.

To manipulate the transmitted acoustic wavefront, a membrane-type acoustic metasurface, which consists of membrane resonators with different side slit thicknesses, as shown in Figure 6(b), can generate transmitted phase shifts covering the full 2π span as shown in Figure 6(c) [60]. As a result, anomalous phenomena, including abnormal sound transmission, acoustic self-bending beam, propagating-to-surface wave conversion, and acoustic focusing [59–61], can be observed in numerical simulations and experiments. Besides, a double-membrane acoustic metasurface was constructed with an air cavity sealed by two elastic membranes, as shown in Figure 6(d) [61]. This study demonstrates that control of the transmission phase shift from 0 to 2π could be realized by adjusting the membrane width, and

propagating waves can be converted into surface waves. Interestingly, a novel thin fibrous membrane with embedded copper beads, which was physically equivalent to cross-linked spring-mass resonators, could also achieve a variety of anomalous functions such as acoustic vortex generation, focusing, and super-resolution [115].

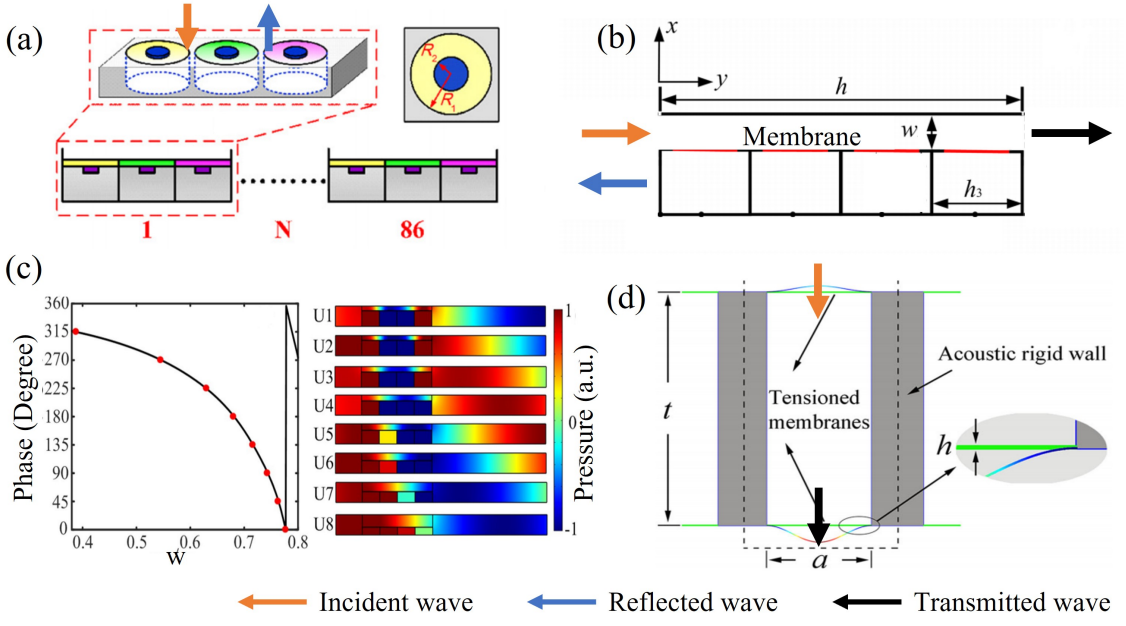

Figure 6: Membrane resonator type of acoustic metasurfaces. (a) Configuration of a membrane resonator. Reprinted from [59], with the permission of AIP Publishing. (b) Membrane type of acoustic metasurface. Reprinted by permission from [60], Copyright 2018 Springer Nature. (c) Transmitted phase shift profile for various slit thickness. Reprinted by permission from [60], Copyright 2018 Springer Nature. (d) Double-membrane resonators. Reprinted by permission from [61], Copyright 2015 Springer Nature.

One challenge is to overcome the geometric complexity and fragility inherent in acoustic metasurfaces with membrane and plate resonators. An alternative and attractive option is to combine several classical materials, for example, porous foams, air gaps, and resonators with this kind of acoustic metasurface [116–118]. Ongoing research is directed towards coupling the acoustic metasurface idea with classical materials, using advanced manufacturing methods. This enables novel combinations of features, such as ultra-thin and ultra-lightweight structures, or adjustable positive/negative bulk modulus and effective density.

3.2.4. Acoustic metasurface with porous materials

Porous materials, which are made of a solid-phase skeleton filled with a fluid phase, can convert sound energy into heat by frictions between the solid structural elements and the fluid phase [119]. The analytical prediction of porous materials' acoustic properties is complicated because of their complicated, often random, internal microstructure [120]. As a result, several empirical models were developed, such as the Delany-Bazley model [121] and Johnson-Champoux-Allard (JCA) model [122–124]. These build links between the macroscopic acoustic properties, such as characteristic impedance and wavenumber, and microstructural parameters, such as porosity, flow resistivity, tortuosity, viscous characteristic length and thermal characteristic length. In the JCA model, the effective bulk modulus K_e and density ρ_e of the rigid frame porous foam can be expressed as:

$$K_e = \frac{\gamma P_0/\phi}{\gamma - \dfrac{\gamma-1}{1+\dfrac{8\eta}{i\Lambda'^2 B^2 \omega\rho_0}\left(1+i\rho_0\dfrac{\omega B^2\Lambda'^2}{16\eta}\right)^{\frac{1}{2}}}}, \tag{11}$$

$$\rho_e = \frac{\beta\rho_0}{\phi}\left[1 + \frac{\sigma\phi}{i\omega\rho_0\beta}\left(1 + \frac{4i\beta^2\eta\rho_0\omega}{\sigma^2\Lambda^2\phi^2}\right)^{\frac{1}{2}}\right], \tag{12}$$

where P_0 and ω are the standard atmospheric pressure and the angular frequency, respectively; η is the viscosity of the fluid phase; γ and ρ_0 are the specific heat ratio and the fluid density, respectively; B^2 is the Prandtl number. Five dominant microstructural parameters in the JCA model are the open porosity ϕ, the flow resistivity σ, the tortuosity β, the viscous characteristic length Λ, and the thermal characteristic length Λ' of the porous material.

Porous acoustic metasurfaces have been proposed to improve the acoustic properties of thin porous materials, where sound energy is trapped and dissipated inside porous elements [125–132]. This broadens the effective bandwidth compared with acoustic metasurfaces made of membrane resonators, Helmholtz resonators, and space-coiling structures. Porous acoustic metasurfaces with intricate rigid geometries inside porous foams have demonstrated excellent sound absorption and sound transmission loss properties with deep sub-wavelength thicknesses, such as porous layers backed by rigid periodic rectangular irregularities [133], porous layers with elaborately inserted rigid partitions (Figure 7(d)) [65], and with rigid resonant inclusions [125].

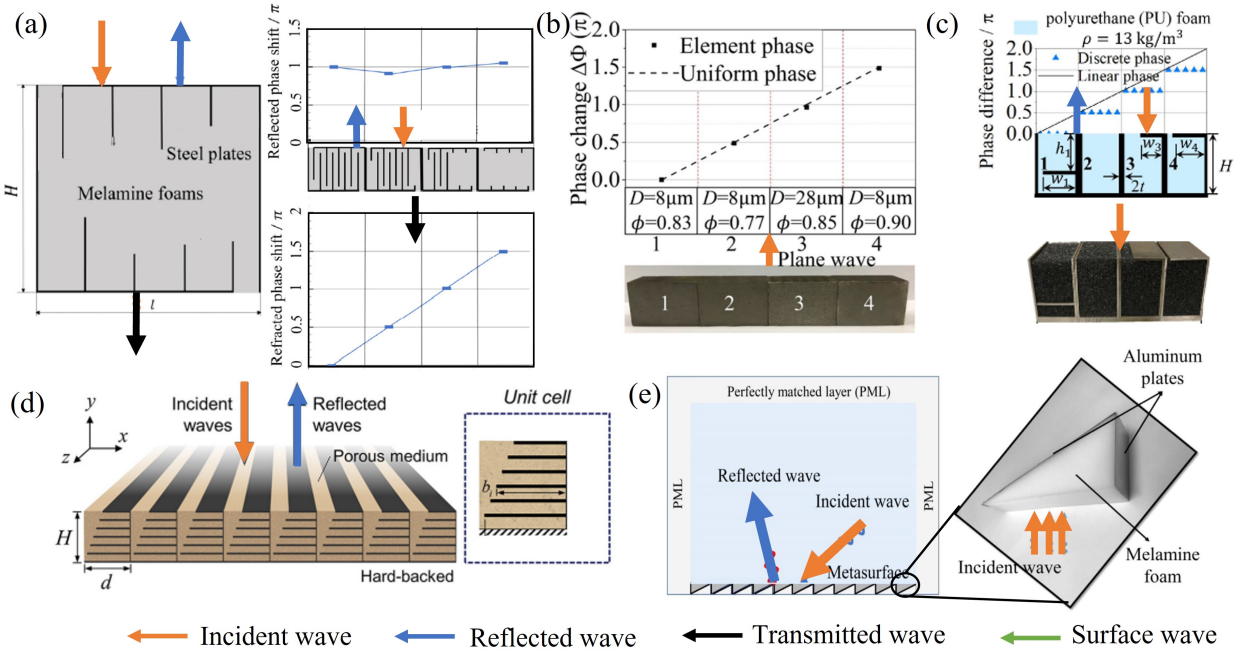

Figure 7: Porous acoustic metasurfaces. (a) Configuration of a typical porous metasurface and its phase shifts. Reprinted from [62], with the permission of AIP Publishing. (b) Metal-based fibrous materials with various fiber diameter and porosity. Reprinted from [63], with the permission of AIP Publishing. (c) Porous metasurface with embedded rigid partitions, Reprinted from [134], Copyright 2019 with permission from Elsevier. (d) Porous layers with elaborately inserted rigid partitions. Reprinted by permission from [65], Copyright 2016 IOP Publishing. (e) Inverted wedge shape porous metasurface. Reprinted from [64], Copyright 2020 with permission from Elsevier.

Porous acoustic metasurfaces provide a method based on the generalized Snell's law to manipulate acoustic waves' propagation and convert propagating waves into surface waves. Desired phase shifts over one periodic length can be obtained by modifying geometrical parameters of the porous elements, including labyrinthine rigid geometry inside porous foams (Figure 7(a)) [62], fiber diameter and material porosity (Figure 7(b)) [63, 135], lengths of embedded rigid partitions (Figure 7(c) and 7(d)) [65, 134], and layer thickness and width (Figure 7(e)) [64, 136]. Anomalous

refraction or reflection phenomena containing high-order wave modes are observed in the scattered sound pressure fields [63]. By adjusting the periodic length, high-order propagating wave modes can be converted to evanescent surface waves [62, 64], significantly improving sound absorption coefficients and transmission loss properties over a wide frequency band.

Sophisticated insertions or structures inside porous foams may be refined to produce state-of-the-art geometrical configurations through topological optimization [106]. The porous acoustic metasurface concept can be extended to various parent materials, most notably soft materials or aerogels, thus reducing their size and weight [137, 138]. Recent research also emphasizes the manufacturing of acoustic metasurfaces as well as control of the acoustic properties. This provides a bridge from theoretical or purely scientific investigations to practical applications [139, 140].

4. Active piezoelectric acoustic metamaterials

In the context of AMs, the term "active" generally refers to AMs with components that can be reconfigured in service or that can exchange energy with acoustic waves, for example extracting electrical energy or providing energy input. The effective frequency range and properties of active AMs can be tuned by several approaches, including piezo-shunting methods [141], fluid-structure interactions [142], mechanical deformation [29, 101, 143, 144], controllable temperature [145, 146], electric fields [147, 148], magnetic fields [149, 150], pressure [146], and adaptive connectivity [151], for multi-functional applications. Specifically, it is our interest to review the current research frontier of active AMs with piezoelectric materials because of their great potential combined with the opportunity for electronic control.

4.1. Physical mechanisms

4.1.1. Piezoelectricity

Piezoelectric materials are solids that accumulate the surface electrical charge under application of external mechanical stress. The piezoelectric effect is defined by a linear interaction between mechanical and electrical fields, and arises due to the lack of inversion symmetry in certain crystalline materials. The converse piezoelectric effect, in which mechanical strain is generated in response to an applied electric field, also occurs in all piezoelectric materials [141]. Active AMs with piezoelectric materials, consisting of mechanical resonators and piezoelectric elements shunted to external circuits, can generate locally resonant bandgaps near the mechanical or electrical resonance. The key benefit of these electromechanical hybrid resonators, compared with passive AMs, is to allow tunable effective mass and stiffness properties. The effective stiffness of one-dimensional [152] and two-dimensional [153] locally resonant piezoelectric AMs have been derived using the Kirchhoff-Love plate theory and the Hamilton's principle.

Pioneering research in active AMs with piezoelectric materials, especially for compound acoustic resonators with piezoelectric membranes as sensors and actuators, was conducted by Akl and Baz analytically and in laboratory tests [21, 23, 24, 154–158]. Piezoelectric materials have also been used in AMs to actuate mechanical deformation, such as bending impedance control and wave propagation tailoring. In addition, by introducing piezoelectric materials into otherwise passive AMs, the effective parameters, including stiffness, bulk modulus and density, could be manipulated through external electronic circuits in real-time over certain frequency bands. Although piezoelectric material implementations of active AMs benefit from the inherent self-sensing characteristic, the brittle nature and high bulk modulus of most piezoelectrics present significant difficulties in practice.

4.1.2. Acoustoelectric interactions

Electron-acoustic wave interaction in piezoelectrics includes three distinct phenomena: gain, acoustoelectric effects, and nonlinear mixing [159]. The fundamental kinds of acoustoelectric interactions, particularly in piezoelectric AMs, are briefly introduced here.

The acoustoelectric effect refers to interactions that occur when an acoustic wave propagates through a piezoelectric material [160]. Acoustic waves travelling through the thickness direction of a piezoelectric layer generate an associated electric field, and thus modify the internal charge distribution [161]. This can release trapped charges, resulting in the generation of an electric signal between neighbouring electrodes [162]. Studies of acoustoelectric interactions indicate that travelling acoustic waves in piezoelectric layers can be attenuated by electron scattering [159, 161, 163]. Conversely, energy can be transferred from moving electrons to the acoustic waves, thereby boosting the energy of the phonons. In general, when the carrier drift velocity exceeds the acoustic velocity, the parallel wave component is enhanced by energy transfer from electrons to phonons, while the anti-parallel wave component is suppressed by electron scattering [159, 163]. Especially for active piezoelectric AMs, when an external circuit is connected across

surface electrodes on a piezoelectric layer, current flows through the external circuit, resulting in a power loss due to the acoustoelectric interaction [161]. Nonlinear acoustoelectric interactions [161] can also occur when acoustic waves propagate through a piezoelectric layer [164, 165]. Harmonic coupling between the acoustic field and a vibrating piezoelectric plate generates strongly coupled electric fields and space-charge waves with periodic electric potential. The charge density is increased by setting the electric field parallel to the wave propagation direction, and power can be transmitted from the acoustic waves to electrons, resulting in attenuation in acoustic energy [159, 163]. The acoustoelectric effect does not appear to have been widely used in generating AMs' anomalous behaviours [166–168].

4.2. Classification

The purpose of this section is to categorise active piezoelectric AMs based on their controllable bulk modulus and effective density. These anomalous physical responses are desirable objectives in the development of novel active materials and structures.

4.2.1. Active piezoelectric AM with tunable effective density

Active piezoelectric AMs are capable of tuning effective density over a range that goes several orders higher and lower than the density of the component materials and can even achieve negative values. More specifically, the piezoelectric elements in active AMs, shunted to external electronic components, allow dynamic tuning of effective density and can thus enhance the operating bandwidth. The tunability comes mainly from the use of acoustoelectric coupling, whereby the effective acoustic properties of piezoelectric elements can be controlled by changes in an external electric circuit linked to electrodes on the piezoelectric material. As a result, anomalous acoustic properties and phenomena, such as negative density and refraction, can be obtained.

The concept of one-dimensional active piezoelectric AMs was proposed based on a multi-cell fluid cavity array with piezoelectric membranes attached on one side of each cavity [21]. The effective density can then be actively tuned by the shunt inductance, passive capacitance, and control voltage. The piezoelectric membranes played a pivotal role in manipulating the stiffness of individual cavities and hence the realization of a frequency-dependent dynamical density over a broad operating frequency range.

A prototype consisting of a water-filled cylindrical pipe sealed by two piezoelectric bimorphs, as shown in Figures 8(a) and 8(b), was proposed to study transmission loss and acoustic impedance numerically and in laboratory tests [154, 169]. The results indicated that the stiffness of the piezoelectric bimorphs could control the cell's homogenized effective density through positive feedback of electrical signals. The positive feedback control loop could be realized by setting one bimorph as a sensor to measure the incident waves and the other one as a control actuator that creates a vibration response consistent with the desired effective density. Then, dynamic density variation by a factor of five or more could be obtained [155]. Furthermore, considering the existence of external disturbances, a disturbance rejection control strategy was applied to accomplish closed-loop control, which could tune the effective density with increasing or decreasing variations along and across the fluid cavity [157].

Membranes and plates with piezoelectric material deposited on both sides have been successfully used to tune their effective properties through external circuits. Using a lead zirconate titanate (PZT) annulus on both sides of a clamped lead membrane, a two-dimensional active piezoelectric AM demonstrated programmable anisotropic density, including both negative and positive density values [158]. A similar plate-type piezoelectric AM made by depositing PZT layers on both sides of brass plates was realized in the lab (Figure 8(c)), confirming controllable effective density [156]. A comparable setup consisting of an ultra-thin aluminium foil bonded with a tunable piezoelectric patch broke the mass law of sound attenuation [172]; this was attributed to the high effective dynamic mass density achieved by adjusting the external piezoelectric circuits.

4.2.2. Active piezoelectric AM with tunable bulk modulus

Piezoelectric components may be integrated into Helmholtz resonator chains in the same way as passive AMs. The piezoelectric element is shunted to external circuits with suitable control strategies to tune their effective bulk modulus. This strategy can extend spatial and spectral controllability of the bulk modulus and structural stiffness.

An active piezoelectric AM with programmable effective bulk modulus was realized for the first time in the water by introducing side Helmholtz resonators that were backed with piezoelectric boundaries into acoustic cavities, as shown in Figure 8(d). The effective bulk modulus of active AMs made of piezoelectric materials was predicted using an analytical approach [23, 170]. A similar active piezoelectric AM with tunable effective bulk modulus was developed by introducing one more piezoelectric Helmholtz resonator onto the opposite side of the acoustic cavity, enabling

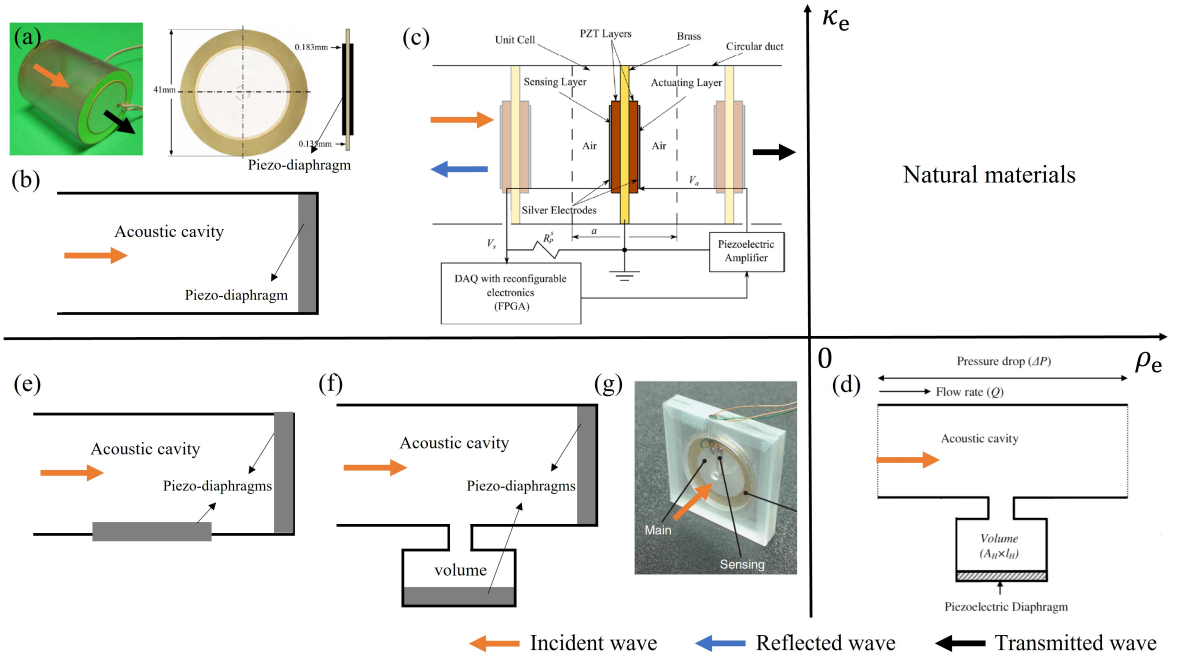

Figure 8: Active AMs with piezoelectric materials. (a) Membranes with programmable negative effective density. Reprinted from [154], with the permission of AIP Publishing. (b) AMs with programmable effective density. (c) Plate-type AMs with programmable effective density. Reprinted from [156], with the permission of AIP Publishing. (d) AMs with programmable bulk modulus. Reprinted by permission from [170], Copyright 2011 IOP Publishing. (e) Double negative AMs with piezoelectric panels on the face of water-filled cylinders. (f) Double negative AMs with piezoelectric panels on the sidewalls of water-filled cylinders. (g) Non-reciprocal and highly nonlinear active AMs. Reprinted by permission from [171], Copyright 2014 Springer Nature.

increased tunability over a broad frequency band. A piezoelectric diaphragm's stiffness may be controlled by adjusting external voltages, resulting in a negative effective bulk modulus [173].

4.2.3. Active piezoelectric AM with double tunable property

Piezoelectric materials can be introduced into membrane or Helmholtz resonator structures in an active piezoelectric AM, whereby their effective density and bulk modulus can be tuned through external electronic control. As in passive AMs, double negative properties can be achieved by periodically side-arranged Helmholtz resonators and elastic layers. Backing these with piezoelectric patches and adjusting external control signals to the piezoelectric elements enable the sound speed and double negativities of the active piezoelectric AMs to be controlled [24].

Active piezoelectric AMs with simultaneously adjustable effective density and bulk modulus have been proposed based on this concept. Figures 8(e) and 8(f) illustrate one approach to achieve this function by placing piezoelectric panels on the faces or sides of water-filled cylinders. Electronic control can then tune the stiffness of the active element so as to modify the homogenized effective bulk modulus and density [24]. An innovative active piezoelectric AM with double negative properties was made using a transducer to sense the incident acoustic waves and a PZT membrane driven by an external electronic circuit for active control. This design allows the effective material properties to be controlled by adjusting external electronics, resulting in tunable effective mass density over a wide range of positive and negative values while the bulk modulus was kept almost constant and vice versa. The active manipulation of negative refraction and tunable absorption property are examples of applications [174]. The piezoelectric membrane could also be coupled with two Helmholtz cavities to form a unidirectional device, as shown in Figure 8(g). With electronic control, this active piezoelectric structure provided tunable local acoustic responses over a relatively broad frequency range. The required phase delay may be established in an array, thus manipulating the direction of transmitted plane waves [27, 171].

The confluence of mechanics, materials, sensing, and control in piezoelectric AMs presents a complex design challenge. The design problem has been addressed by a number of researchers [27, 153, 175–179]. Active piezoelectric AMs have an even larger number of design variables and functional goals. In this context, machine learning approaches can assist in data analysis to uncover optimum solutions [180, 181]. Beyond the technical challenges listed here, a requirement for realizing such a long-term vision is to collaborate on innovations that span materials science, mechanical and electrical engineering, manufacturing, and other fields.

4.3. Applications

Extraordinary acoustic properties can be obtained through active piezoelectric AMs, resulting in a variety of benefits, including a new class of ultra-lightweight and ultra-thin structures, negative sound reflection and refraction, controllable and tunable effective bulk modulus and density, energy harvesting, and noise reduction. Furthermore, active piezoelectric AMs provide a way to realize multiple functions, such as anomalous reflection, refraction and focusing, sound isolation, and acoustic cloaking, using only one acoustic device with varying external control circuits.

4.3.1. Wave manipulation

Tailoring acoustic wavefront into a desired direction or shape has attracted tremendous attention in the field of passive AMs. This function relies on the Huygens–Fresnel principle [93], where sound fields can be formed by a sum of spherical wavelets generated by the active piezoelectric AMs.

An active piezoelectric AM with an ultra-thin hybrid membrane was fabricated by depositing a PZT annulus on both sides of low-density polythene membranes attached with steel masses. Adjustable transmitted phase shifts of acoustic waves could be realized by tuning external static voltages in real-time. The phase shift mechanism relied on the change of tension, stiffness and mass of the membranes, which could be manipulated using the piezoelectric layers [182]. To control reflected acoustic waves, a comparable active AM with piezoelectric transducers and lead layers was developed in Figure 9(a) [183]. Anomalous transmission and reflection phenomena, including acoustic cloaking (Figure 9(c)), wave manipulation (Figure 9(d)), and self-bending beams (Figure 9(e)), could be realized electrically rather than requiring a different mechanical configuration [182, 183]. For surface acoustic waves, anomalous wave conversion from incident surface waves into bulk shear waves could also be actively manipulated by utilizing piezoelectric units [184].

Tunable acoustic waveguides typically comprise a thin plate with periodic cylindrical stubs and a series of piezoelectric transducers with external circuits, as shown in Figure 9(f) [141]. The piezoelectric transducer's resonance characteristics lead to strong response at specific frequencies, enabling abnormal phenomena such as wave mode conversions. In general, active AMs with piezoelectric materials enable the design of multi-functional structures capable of performing a range of wave manipulation functions with a single device [141, 183–187].

4.3.2. Energy harvesting

Acoustic energy harvesters are devices that convert acoustic energy into electrical energy. Piezoelectricity is one of the typical approaches to harvest acoustic energy, where the energy conversion efficiency strongly depends on the elastic, piezoelectric and dielectric properties of the piezoelectric material. Natural bulk materials are limited by their intrinsic physical properties, but active piezoelectric AMs provide a way to extend material properties to values that are not normally available, such as negative stiffness, density, and refractive index. By introducing active piezoelectric AMs into acoustic energy harvesting devices, their anomalous physical properties lead to innovative mechanisms to further improve energy conversion efficiency. Two main ways of using piezoelectric AMs to enhance energy harvesting have been proposed: concentration of acoustic energy and resonance effects.

The first approach, confinement, can be achieved by introducing a sub-wavelength defect into a two-dimensional lattice structure of meta-atoms [188, 198–201]. As shown in Figures 10(a) and 10(b), when an incident acoustic wave hits the AM, the sound energy can be confined into the sub-wavelength defect. Then a piezoelectric patch can be placed at the defect position to harvest acoustic energy. The interaction between the piezoelectric AM and acoustic waves can be described analytically by ignoring the mass and stiffness of the piezoelectric element [188]. It indicated that the operating frequency could be adjusted by modifying the properties of the meta-atoms. To improve energy conversion efficiency, this model examined sub-wavelength flaws of different sizes and types. Another approach is using an acoustic metasurface to concentrate incident acoustic energy in a spatial point and then collect the focused acoustic energy through piezoelectric materials [189, 202–204]. A passive acoustic metasurface with a labyrinthine structure was utilized to focus incident acoustic waves at a spatial point, where a piezoelectric bimorph was placed to

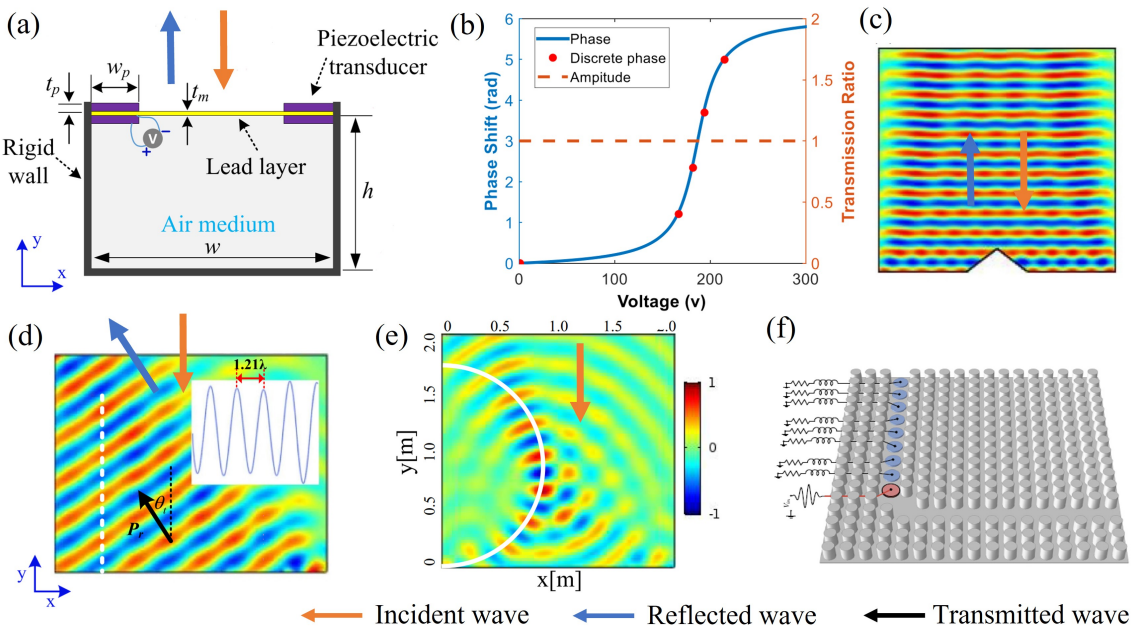

Figure 9: Applications of Active piezoelectric AMs in wave manipulation. (a) Membrane type of active piezoelectric AMs. Reprinted by permission from [183], Copyright 2020 IOP Publishing. (b) Phase shift and corresponding static voltage. Reprinted by permission from [183], Copyright 2020 IOP Publishing. (c) Acoustic cloaking, Reprinted by permission from [183], Copyright 2020 IOP Publishing. (d) Anomalous wave manipulation. Reprinted by permission from [183], Copyright 2020 IOP Publishing. (e) Nonparaxial beam generation. Reprinted by permission from [183], Copyright 2020 IOP Publishing. (f) Tunable acoustic waveguide. Reprinted from [141], with the permission of AIP Publishing.

collect acoustic energy, as shown in Figure 10(c). The numerical results indicated that the output voltage and power obtained by the piezoelectric bimorph dramatically increased with the use of the acoustic metasurface [202, 203].

The second approach to energy harvesting is through embedding piezoelectric materials into AMs with deep sub-wavelength sizes for low-frequency incident acoustic waves [190–197, 205–210]. By placing a beam-based PZT transducer inside a cavity sealed by two mass-attached membranes, the collected acoustic energy could be significantly increased, as shown in Figure 10(d). When the first resonance of the PZT transducer is close to the resonance of the membrane-type meta-atom, maximum sound pressure amplification and a dramatic enhancement of energy harvesting were found both experimentally and in numerical simulations [190]. Similarly, a pre-stretched polyurethane membrane with two rigid mass sheets attached on both sides (Figure 10(e)) exhibited energy harvesting capability using piezoelectric patches [191]. An acoustoelastic AM, consisting of a rectangular aluminium frame and a cylindrical matrix with a massive spherical core, was proposed to convert the trapped strain energy into electrical energy through piezoelectric wafers inside the matrix, as shown in Figure 10(f). The unit could be modelled as a conventional spring-mass system, where the core mass, placement of piezoelectric wafers and coupling resonance effects determine the energy harvesting efficiency [192, 209, 210]. At low frequencies, significant sound amplification was obtained in a double-wall labyrinthine AM in Figure 10(m). In comparison to a typical bimorph plate, the coupling between the AM structure and the piezoelectric bimorph plate significantly increased the output voltage [197].

Numerous active piezoelectric AM structures have been explored to improve output power at low frequencies while also reducing device size. Typical optimizations include altering the membrane material (Figure 10(g)) [193], including Helmholtz resonators (Figure 10(h)) [194, 205], constructing tortuous structures with narrow channels (Figure 10(j)) [195], and fabricating acoustic resonators with bonded piezoelectric patches (Figure 10(k)) [196, 206–208]. A performance summary of acoustic energy harvesters using active AMs with piezoelectric effects is listed in Table 2. It can be seen that attaining tunability and a wide bandwidth, as well as good energy conversion efficiency and a compact device size, continue to be challenging. By introducing active piezoelectric AMs, some constraints of conventional piezoelectric materials in terms of material properties, device size, and coupling efficiencies can

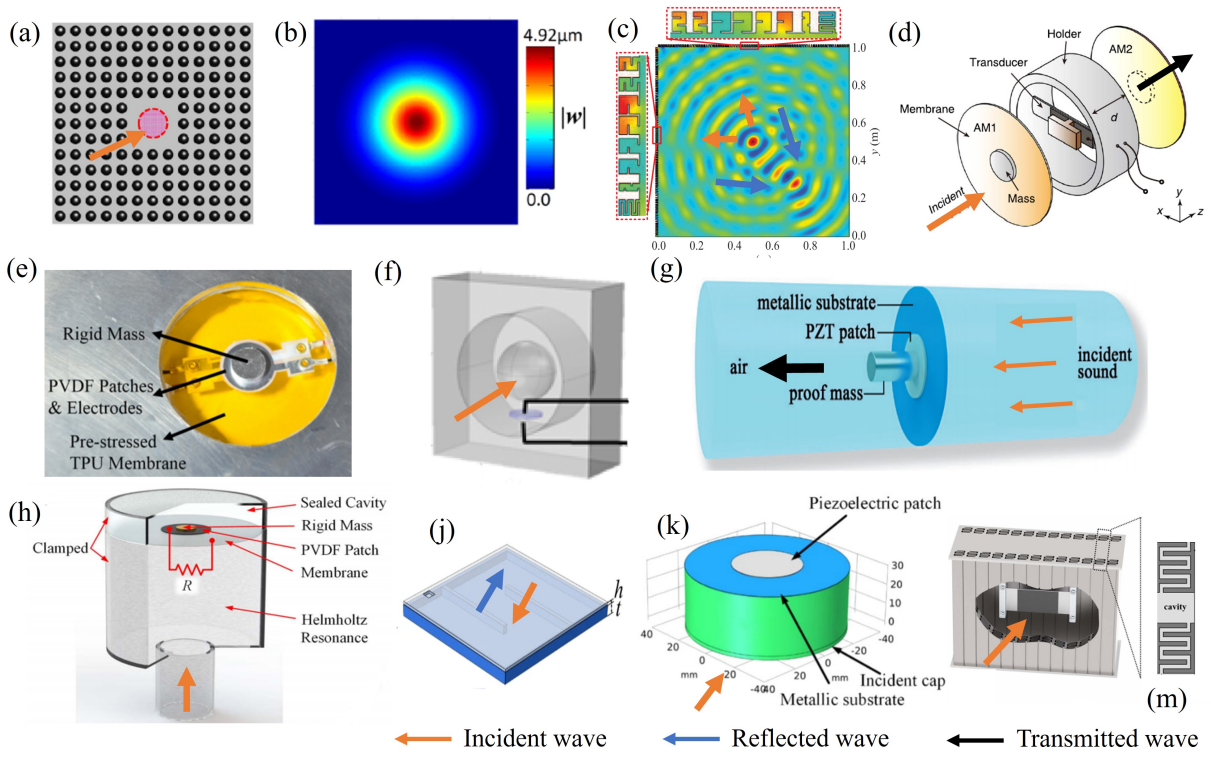

Figure 10: Acoustic energy harvesters by utilizing AMs with piezoelectric effects. (a) Acoustic metasurface with sub-wavelength defects. Reprinted by permission from [188], Copyright 2017 IOP Publishing. (b) Acoustic energy focused at a sub-wavelength defect. Reprinted by permission from [188], Copyright 2017 IOP Publishing. (c) Acoustic energy harvesting by passive labyrinthine AMs. Reprinted figure with permission from [189], Copyright 2017 by the American Physical Society. (d) AM made of a cavity sealed by two membranes. Reprinted by permission from [190], Copyright 2017 IOP Publishing. (e) AM with a re-stretched membrane. Reprinted by permission from [191], Copyright 2016 IOP Publishing. (f) AM consisting of a rectangular frame, a cylindrical matrix and a heavy core. Reprinted from [192], with the permission of AIP Publishing. (g) Metallic-based membrane type of AM. Reprinted by permission from [193], Copyright 2016 IOP Publishing. (h) AM with a membrane inside a Helmholtz resonator. Reprinted by permission from [194], Copyright 2018 IOP Publishing. (j) Foldy-structured metasurface with narrow channels. Reprinted by permission from [195], Copyright 2019 Springer Nature. (k) Compact acoustic energy harvester. Reprinted by permission from [196], Copyright 2020 IOP Publishing. (m) Double-wall labyrinthine structure. Reprinted by permission from [197], Copyright 2017 IOP Publishing.

be overcome. This enables the development of multi-functional active piezoelectric AM structures capable of wave manipulation, energy harvesting, and noise reduction.

4.3.3. Noise reduction

Passive AMs have demonstrated excellent acoustic performance over the desired frequency range as acoustic liners in the past twenty years, achieving enhanced transmission loss and breaking the mass law. However, a challenge still remains in the trade-off challenge between effective bandwidth, efficiency, and device size. By incorporating active piezoelectric elements into passive AMs, such as space coiling structures, Helmholtz resonators, and membrane resonators, higher sound absorption or transmission coefficients can be reached over a wide tunable frequency range, with a deep sub-wavelength device size.

For applications of active piezoelectric AMs in noise reduction, a sandwich structure, where multiple sub-wavelength shunted piezoelectric patches were bonded to a thin plate (Figure 11(a)), was investigated using the effective medium method [175, 211] and numerical simulations [175, 212]. The findings show that active AMs with shunted piezoelectric patches may achieve much higher sound transmission losses and a considerably wider effective bandwidth [175] than classical materials of comparable size and weight. The sound transmission loss of a similarly

Table 2
Summary of AMs applied in piezoelectric energy harvesting (NG: Not Given).

Reference	Device size/cm^3	SPL/dB	Frequency/Hz	Voltage/V	Power output/μW	Energy density/μWcm^{-3}
Qi [198]	18	100	2257.5	1.3	8.8	0.54
Oudich [188]	23	100	520	0.45	18	0.78
Qi [202]	NG	NG	3430	4	12	NG
Sun [197]	NG	100	600	0.2585	0.345	NG
Sun [202]	251	100	183	NG	7.3	0.029
Yuan [208]	200	100	341	NG	66.7	0.33
Yuan [193]	98	114	155	9	210	2.14
Zhang [194]	155	94	453	0.413	3.22	0.02
Jin [195]	NG	100	1303	4.4	8.6	NG
Eghbali [206]	NG	100	107	NG	44	NG
Ma [200]	36	120	3086	0.291	28	0.77
Yuan [196]	41	100	140	NG	8.1	0.19

active piezoelectric AM in Figure 11(b), by substituting the thin plate in Figure 11(a) with an acoustic cavity, was evaluated using a fully-coupled analytical model based on the plate theory [176]. The numerical simulation was used to investigate the impact of acoustic cavity depth, external voltages, incident wave orientations, and gas and material types on the sound transmission loss. A tunable acoustic metasurface in Figure 11(c) was made using an array of beam steering devices, as shown in Figure 8(g), which could be configured to simultaneously implement various functions by adjusting external electronics rather than changing the physical structures [27].

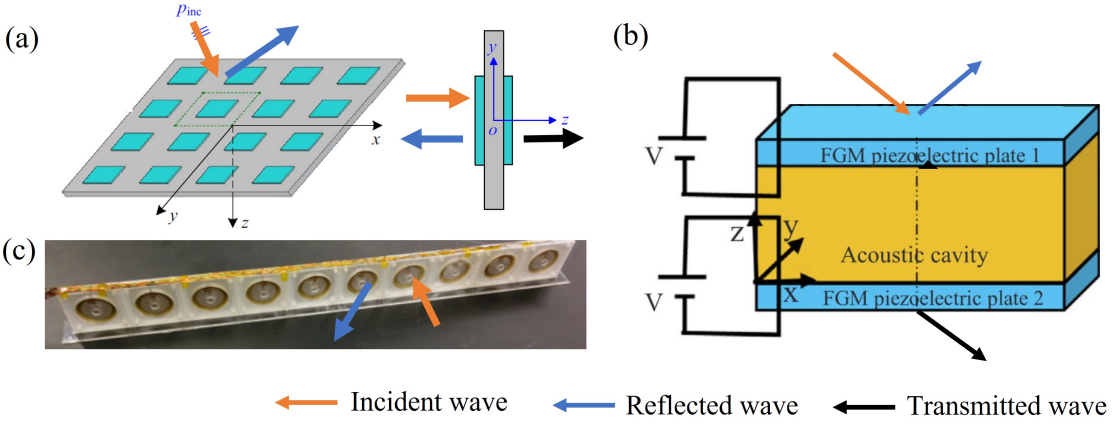

Figure 11: Active piezoelectric AMs with applications in noise reduction. (a) Schematic diagram of AMs with shunted piezoelectric patches, Reprinted from [175], Copyright 2015 with permission from Elsevier. (b) Piezoelectric plates with an acoustic cavity. Reprinted from [176], Copyright 2019 with permission from Elsevier. (c) An array consisting of ten active cells. Reprinted figure with permission from [27], Copyright 2015 by the American Physical Society.

In general, incorporating piezoelectric materials into AMs enables the creation of novel active piezoelectric AMs with a tunable effective frequency range. Active piezoelectric AMs exhibit a variety of extraordinary acoustic properties, many of which are not found in conventional materials, and therefore have a broad range of potential applications. Detailed comparisons of passive AMs and active piezoelectric AMs are given in Table 3.

Current active piezoelectric AMs have relied significantly on manufacturing methods to demonstrate different functions in the laboratory, with the success and quality of the resulting structures being highly dependent on the operating procedure and material properties [27, 153, 176–179]. In addition, sensing, actuation, and digital controller components should be precisely and repeatably integrated within active piezoelectric AMs. Finally, it should be noted

Table 3
Comparisons of passive AMs and active piezoelectric AMs.

Type of AMs	Applications	Characteristics in structure and performance
Sub-wavelength meta-atoms	Complete sound insulation and absorption, wave manipulation (negative refraction and reflection).	Deep sub-wavelength size, single-item structure. & Negative properties, fixed and narrow effective frequency range.
Space coiling structures	Complete sound insulation and absorption, wave manipulation (negative refraction and reflection, propagating-to-surface-wave conversion, acoustic focusing, one-way propagation, acoustic vortex generation, cloaking).	Deep sub-wavelength size, topological optimization, complexity in structure. & Negative properties, fixed and narrow effective frequency range.
Helmholtz resonators	Complete sound insulation and absorption, wave manipulation (negative refraction and reflection, propagating-to-surface-wave conversion, acoustic focusing, one-way propagation, cloaking).	Deep sub-wavelength size, ease of fabrication. & Negative properties, fixed and narrow frequency range.
Membrane and plate resonators	Complete sound insulation and absorption, wave manipulation (negative refraction and reflection, propagating-to-surface-wave conversion, acoustic focusing, acoustic vortex generation, super resolution, cloaking).	Deep sub-wavelength size, geometric complexity and fragility, lightweight. & Negative properties, fixed and narrow effective frequency range.
Porous materials	Excellent sound attenuation, wave manipulation (negative refraction and reflection, propagating-to-surface-wave conversion).	Deep sub-wavelength size, ease of fabrication, lightweight. & Negative properties, broadband effective frequency range.
Active piezoelectric AMs	Complete sound insulation and absorption, wave manipulation (negative refraction and reflection, propagating-to-surface-wave conversion, acoustic focusing), energy harvesting.	Extremely deep sub-wavelength size, ease of fabrication. & Negative properties, tunable effective frequency range, multi-functional potential, electronic control.

that although the development of active piezoelectric AMs is still in its early stages, it is prudent for researchers to look ahead and consider possible applications.

5. Conclusions and outlook

5.1. Conclusions

The field of acoustic metamaterials and metasurfaces has rapidly grown over the past twenty years. The anomalous material properties of AMs have been regarded as a breakthrough beyond the properties of conventional materials, which potentially enables many advances. Exciting prospects in physical and engineering applications have been proposed, such as sound absorbers and insulators, wave manipulation, cloaking, energy harvesting, communications, imaging, and medical devices with improved performance and reduced size or weight.

However, there still exist significant challenges limiting the practical applications of AMs. Initially, AMs were passive structures, and their main drawback lay in inherently narrow bandgaps. In other words, the effective frequency range with anomalous performance was narrow and determined by structural resonance. Additionally, in passive AMs, the engineered sub-wavelength structures indicate high dissipation at the resonance frequency causing high energy loss. Furthermore, passive AMs are not adaptable to changes in working conditions or environment: their unique characteristics remain constant, being in strict accordance with designed-in structural parameters. As a result, the extraordinary performance cannot be controlled or optimized in varying service conditions. Finally, a number of AMs, such as passive membrane resonators, require structural complexity that tends to result in fragility and is a challenge for fabrication. Active piezoelectric AMs offer the opportunity of extraordinary material properties with adjustable frequency bands. For instance, piezoelectric elements introduced into membrane-type or Helmholtz-resonator-type AMs create a mechanism for electronic control and feedback. The dynamic density or modulus of the active piezoelectric AMs can then be modified, resulting in negative reflection and refraction over variable and controllable frequency bands. Much current research focuses on the use of adaptive external circuits to achieve

adjustable frequency, with conventional PZT materials widely adopted as the active piezoelectric elements. However, there is still potential for substantial improvement of active piezoelectric AMs. The commonly used piezoelectric materials have acceptable acoustic impedance matching with water but poor matching with air, resulting in acoustic energy leakage into undesired wave modes. As a result, there is a trade-off relating efficiency, frequency range, device size, and capability for wavefront manipulation in current active piezoelectric AMs. Truly broad-band wave manipulation with high efficiency has yet to be achieved in practical devices.

5.2. Outlook

The potential applications in acoustic energy harvesting, anomalous wave manipulation, and noise reduction are driving rapid research progress in AMs. Noise reduction seems to be one of the most promising applications. Given the limits of passive AMs, the development of active piezoelectric AMs for a variety of applications is motivated by the need to increase effective bandwidth, adjust operating frequency, and reduce size and weight.

In recent years, soft and porous AMs which utilize their porous structure to broaden effective bandgaps are gaining research interest. Fibrous materials, effectively a type of open-cell porous foam, allow ease of density manipulation by adjusting fiber diameters and packing [213–220]. This approach can provide improved impedance matching with air. Similarly, soft materials such as hydrogels [221], elastomers [222], aerogel [131], and soft fiber/bead composites [115] have been used to realize AMs that are well-matched to air. Bubble crystals, which are representative of soft AMs in water, have shown attractive bandgaps in analysis [223, 224] and experiments [138, 225]. Using effective methods for analyzing bubbles and foams [226], bubble AMs have great potential for wave manipulation applications, such as underwater total reflection, insulation and cloaking [227–229], and enhanced water-air acoustic transmission [230]. Inspired by passive AMs, active soft AMs based on fibrous piezoelectric materials may potentially broaden and tune effective bandgaps simultaneously in the future. However, the development of active fibrous piezoelectric AMs is still in its early phases, so researchers face the challenge of making choices among physical mechanisms and optimising technical performance within the limitations imposed by fabrication methods.

The development of multi-functional active piezoelectric AMs is an exciting new research direction, whereby a single structure may achieve distinct metamaterial effects under external electronic control. These are highly engineered materials with complex structures, presenting a challenge for manufacture. The recent rapid development of additive manufacturing technology provides an opportunity to fabricate the required complex structures with advantageous properties, including the opportunity to mix piezoelectric and polymer materials. The influence of temperature, humidity, external flow, curvature on the structure, and material properties all need to be considered in future active piezoelectric AM designs. Considering the vast progress achieved over the past decade, AMs and active piezoelectric AMs have matured rapidly and seem likely to make a substantial impact in engineering applications in the near future.

Acknowledgments

Guosheng Ji is supported by the Clarendon Fund and Trinity College Scholarship at the University of Oxford.

References

[1] R. M. Walser, “Electromagnetic metamaterials,” in *International Symposium on Optical Science and Technology*, International Society for Optics and Photonics, 2001.

[2] M. A. Noginov and V. A. Podolskiy, *Tutorials in metamaterials*. CRC press, 2011.

[3] V. G. Veselago, “The electrodynamics of substances with simultaneously negative values of ϵ and μ,” *Soviet Physics Uspekhi*, vol. 10, no. 4, p. 509, 1968.

[4] J. Pendry, A. Holden, W. Stewart, and I. Youngs, “Extremely low frequency plasmons in metallic mesostructures,” *Physical Review Letters*, vol. 76, no. 25, p. 4773, 1996.

[5] J. B. Pendry, A. Holden, D. Robbins, and W. Stewart, “Magnetism from conductors and enhanced nonlinear phenomena,” *IEEE Transactions on Microwave Theory and Techniques*, vol. 47, no. 11, pp. 2075–2084, 1999.

[6] D. R. Smith, W. J. Padilla, D. Vier, S. C. Nemat-Nasser, and S. Schultz, “Composite medium with simultaneously negative permeability and permittivity,” *Physical Review Letters*, vol. 84, no. 18, p. 4184, 2000.

[7] R. A. Shelby, D. R. Smith, and S. Schultz, “Experimental verification of a negative index of refraction,” *Science*, vol. 292, no. 5514, pp. 77–79, 2001.

[8] J. Valentine, S. Zhang, T. Zentgraf, E. Ulin-Avila, D. A. Genov, G. Bartal, and X. Zhang, “Three-dimensional optical metamaterial with a negative refractive index,” *Nature*, vol. 455, no. 7211, pp. 376–379, 2008.

[9] P. Moitra, Y. Yang, Z. Anderson, I. I. Kravchenko, D. P. Briggs, and J. Valentine, “Realization of an all-dielectric zero-index optical metamaterial,” *Nature Photonics*, vol. 7, no. 10, pp. 791–795, 2013.

[10] N. Yu, P. Genevet, M. A. Kats, F. Aieta, J. P. Tetienne, F. Capasso, and Z. Gaburro, "Light propagation with phase discontinuities: generalized laws of reflection and refraction," *Science*, no. 6054, 2011.

[11] Z. Liu, X. Zhang, Y. Mao, Y. Zhu, Z. Yang, C. Chan, and P. Sheng, "Locally resonant sonic materials," *Science*, vol. 289, no. 5485, pp. 1734–1736, 2000.

[12] Y. Li, B. Liang, Z. M. Gu, X. Zou, and J. C. Cheng, "Reflected wavefront manipulation based on ultrathin planar acoustic metasurfaces," *Scientific Reports*, 2013.

[13] X. Xiao, Z. He, E. Li, B. Zhou, and X. Li, "A lightweight adaptive hybrid laminate metamaterial with higher design freedom for wave attenuation," *Composite Structures*, vol. 243, p. 112230, 2020.

[14] K. Yi and M. Collet, "Broadening low-frequency bandgaps in locally resonant piezoelectric metamaterials by negative capacitance," *Journal of Sound and Vibration*, vol. 493, p. 115837, 2021.

[15] X. Shen, C. Jiang, Y. Li, and J. Huang, "Thermal metamaterial for convergent transfer of conductive heat with high efficiency," *Applied Physics Letters*, vol. 109, no. 20, p. 201906, 2016.

[16] T. Han, X. Bai, D. Liu, D. Gao, B. Li, J. T. Thong, and C. W. Qiu, "Manipulating steady heat conduction by sensu-shaped thermal metamaterials," *Scientific Reports*, vol. 5, no. 1, pp. 1–7, 2015.

[17] F. Chen and D. Y. Lei, "Experimental realization of extreme heat flux concentration with easy-to-make thermal metamaterials," *Scientific Reports*, vol. 5, no. 1, pp. 1–8, 2015.

[18] A. Movchan and S. Guenneau, "Split-ring resonators and localized modes," *Physical Review B*, vol. 70, no. 12, p. 125116, 2004.

[19] J. Li and C. Chan, "Double-negative acoustic metamaterial," *Physical Review E*, vol. 70, no. 5, p. 055602, 2004.

[20] N. Fang, D. Xi, J. Xu, M. Ambati, W. Srituravanich, C. Sun, and X. Zhang, "Ultrasonic metamaterials with negative modulus," *Nature Materials*, vol. 5, no. 6, pp. 452–456, 2006.

[21] A. Baz, "The structure of an active acoustic metamaterial with tunable effective density," *New Journal of Physics*, vol. 11, no. 12, p. 123010, 2009.

[22] S. H. Lee, C. M. Park, Y. M. Seo, Z. G. Wang, and C. K. Kim, "Composite acoustic medium with simultaneously negative density and modulus," *Physical Review Letters*, vol. 104, no. 5, p. 054301, 2010.

[23] W. Akl and A. Baz, "Multi-cell active acoustic metamaterial with programmable bulk modulus," *Journal of Intelligent Material Systems and Structures*, vol. 21, no. 5, pp. 541–556, 2010.

[24] W. Akl and A. Baz, "Active acoustic metamaterial with simultaneously programmable density and bulk modulus," *Journal of Vibration and Acoustics*, vol. 135, no. 3, 2013.

[25] F. Aieta, A. Kabiri, P. Genevet, N. Yu, M. A. Kats, Z. Gaburro, and F. Capasso, "Reflection and refraction of light from metasurfaces with phase discontinuities," *Journal of Nanophotonics*, vol. 6, no. 1, pp. 063532–063532, 2012.

[26] Y. Li, X. Jiang, R. Q. Li, B. Liang, X. Y. Zou, L. L. Yin, and J. C. Cheng, "Experimental realization of full control of reflected waves with subwavelength acoustic metasurfaces," *Physical Review Applied*, vol. 2, no. 6, p. 064002, 2014.

[27] B. I. Popa, D. Shinde, A. Konneker, and S. A. Cummer, "Active acoustic metamaterials reconfigurable in real time," *Physical Review B*, vol. 91, no. 22, p. 220303, 2015.

[28] F. Ju, W. Xiong, C. Liu, Y. Cheng, and X. Liu, "Acoustic accelerating beam based on a curved metasurface," *Applied Physics Letters*, vol. 114, no. 11, p. 113507, 2019.

[29] X. S. Li, Y. F. Wang, A. L. Chen, and Y. S. Wang, "An arbitrarily curved acoustic metasurface for three-dimensional reflected wave-front modulation," *Journal of Physics D: Applied Physics*, vol. 53, no. 19, p. 195301, 2020.

[30] G. Ma and P. Sheng, "Acoustic metamaterials: From local resonances to broad horizons," *Science Advances*, vol. 2, no. 2, p. e1501595, 2016.

[31] S. A. Cummer, J. Christensen, and A. Alù, "Controlling sound with acoustic metamaterials," *Nature Reviews Materials*, vol. 1, no. 3, pp. 1–13, 2016.

[32] J. Liu, H. Guo, and T. Wang, "A review of acoustic metamaterials and phononic crystals," *Crystals*, vol. 10, no. 4, p. 305, 2020.

[33] B. Assouar, B. Liang, Y. Wu, Y. Li, J.-C. Cheng, and Y. Jing, "Acoustic metasurfaces," *Nature Reviews Materials*, vol. 3, no. 12, pp. 460–472, 2018.

[34] X. Zhang, Z. Qu, and H. Wang, "Engineering acoustic metamaterials for sound absorption: From uniform to gradient structures," *Iscience*, vol. 23, no. 5, p. 101110, 2020.

[35] S. Kumar and H. P. Lee, "Recent advances in acoustic metamaterials for simultaneous sound attenuation and air ventilation performances," *Crystals*, vol. 10, no. 8, p. 686, 2020.

[36] S. Kumar and H. P. Lee, "The present and future role of acoustic metamaterials for architectural and urban noise mitigations," in *Acoustics*, vol. 1, pp. 590–607, Multidisciplinary Digital Publishing Institute, 2019.

[37] G. Liao, C. Luan, Z. Wang, J. Liu, X. Yao, and J. Fu, "Acoustic metamaterials: A review of theories, structures, fabrication approaches, and applications," *Advanced Materials Technologies*, vol. 6, no. 5, p. 2000787, 2021.

[38] Q. Chen, B. Zhang, Y. Bai, L. Wang, and M. Rejab, "Review of phononic crystals and acoustic metamaterials," in *IOP Conference Series: Materials Science and Engineering*, vol. 788, p. 012052, IOP Publishing, 2020.

[39] S. Kumar and H. Pueh Lee, "Recent advances in active acoustic metamaterials," *International Journal of Applied Mechanics*, vol. 11, no. 08, p. 1950081, 2019.

[40] S. Chen, Y. Fan, Q. Fu, H. Wu, Y. Jin, J. Zheng, and F. Zhang, "A review of tunable acoustic metamaterials," *Applied Sciences*, vol. 8, no. 9, p. 1480, 2018.

[41] F. Zangeneh Nejad and R. Fleury, "Active times for acoustic metamaterials," *Reviews in Physics*, vol. 4, p. 100031, 2019.

[42] T. J. Cox and P. D'Antonio, *Acoustic absorbers and diffusers: theory, design and application*. CRC Press, 2009.

[43] G. Ma, M. Yang, S. Xiao, Z. Yang, and P. Sheng, "Acoustic metasurface with hybrid resonances," *Nature Materials*, vol. 13, no. 9, pp. 873–878, 2014.

[44] F. Ma, Y. Xu, and J. H. Wu, "Shell-type acoustic metasurface and arc-shape carpet cloak," *Scientific Reports*, vol. 9, no. 1, pp. 1–11, 2019.

[45] J. Jin Park, J. H. Kwak, and K. Song, "Ultraslow medium with an acoustic membrane-like undamped dynamic vibration absorber for low-frequency isolation," *Extreme Mechanics Letters*, p. 101203, 2021.

[46] M. F. Limonov, M. V. Rybin, A. N. Poddubny, and Y. S. Kivshar, "Fano resonances in photonics," *Nature Photonics*, vol. 11, no. 9, pp. 543–554, 2017.

[47] C. Ding, L. Hao, and X. Zhao, "Two-dimensional acoustic metamaterial with negative modulus," *Journal of Applied Physics*, vol. 108, no. 7, p. 074911, 2010.

[48] V. M. Garcia-Chocano, R. Graciá-Salgado, D. Torrent, F. Cervera, and J. Sánchez-Dehesa, "Quasi-two-dimensional acoustic metamaterial with negative bulk modulus," *Physical Review B*, vol. 85, no. 18, p. 184102, 2012.

[49] Z. Liang, T. Feng, S. Lok, F. Liu, K. B. Ng, C. H. Chan, J. Wang, S. Han, S. Lee, and J. Li, "Space-coiling metamaterials with double negativity and conical dispersion," *Scientific Reports*, vol. 3, p. 1614, 2013.

[50] Y. Xie, B. I. Popa, L. Zigoneanu, and S. A. Cummer, "Measurement of a broadband negative index with space-coiling acoustic metamaterials," *Physical Review Letters*, vol. 110, no. 17, p. 175501, 2013.

[51] Y. F. Wang, Y. S. Wang, and C. Zhang, "Two-dimensional locally resonant elastic metamaterials with chiral comb-like interlayers: Bandgap and simultaneously double negative properties," *The Journal of the Acoustical Society of America*, vol. 139, no. 6, pp. 3311–3319, 2016.

[52] Y. Xie, W. Q. Wang, H. Y. Chen, A. Konneker, B. I. Popa, and S. A. Cummer, "Wavefront modulation and subwavelength diffractive acoustics with an acoustic metasurface," *Nature Communications*, 2014.

[53] H. Esfahlani, H. Lissek, and J. R. Mosig, "Generation of acoustic helical wavefronts using metasurfaces," *Physical Review B*, vol. 95, no. 2, p. 024312, 2017.

[54] C. Ding, H. Chen, S. Zhai, S. Liu, and X. Zhao, "The anomalous manipulation of acoustic waves based on planar metasurface with split hollow sphere," *Journal of Physics D: Applied Physics*, vol. 48, no. 4, p. 045303, 2015.

[55] J. Lan, Y. Li, Y. Xu, and X. Liu, "Manipulation of acoustic wavefront by gradient metasurface based on helmholtz resonators," *Scientific Reports*, vol. 7, no. 1, pp. 1–9, 2017.

[56] J. Guo, X. Zhang, Y. Fang, and R. Fattah, "Reflected wave manipulation by inhomogeneous impedance via varying-depth acoustic liners," *Journal of Applied Physics*, vol. 123, no. 17, p. 174902, 2018.

[57] K. Song, J. Kim, S. Hur, J. H. Kwak, S. H. Lee, and T. Kim, "Directional reflective surface formed via gradient-impeding acoustic meta-surfaces," *Scientific Reports*, vol. 6, p. 32300, 2016.

[58] J. Li, C. Shen, A. Díaz-Rubio, S. A. Tretyakov, and S. A. Cummer, "Systematic design and experimental demonstration of bianisotropic metasurfaces for scattering-free manipulation of acoustic wavefronts," *Nature Communications*, vol. 9, no. 1, pp. 1–9, 2018.

[59] X. Chen, P. Liu, Z. Hou, and Y. Pei, "Implementation of acoustic demultiplexing with membrane-type metasurface in low frequency range," *Applied Physics Letters*, vol. 110, no. 16, p. 161909, 2017.

[60] J. Lan, X. Zhang, X. Liu, and Y. Li, "Wavefront manipulation based on transmissive acoustic metasurface with membrane-type hybrid structure," *Scientific Reports*, vol. 8, no. 1, pp. 1–9, 2018.

[61] S. Zhai, H. Chen, C. Ding, F. Shen, C. Luo, and X. Zhao, "Manipulation of transmitted wave front using ultrathin planar acoustic metasurfaces," *Applied Physics A*, vol. 120, no. 4, pp. 1283–1289, 2015.

[62] G. Ji, Y. Fang, J. Zhou, and X. Huang, "Porous labyrinthine acoustic metamaterials with high transmission loss property," *Journal of Applied Physics*, vol. 125, no. 21, p. 215110, 2019.

[63] Y. Fang, X. Zhang, and J. Zhou, "Sound transmission through an acoustic porous metasurface with periodic structures," *Applied Physics Letters*, vol. 110, no. 17, p. 171904, 2017.

[64] G. Ji, Y. Fang, and J. Zhou, "Porous acoustic metamaterials in an inverted wedge shape," *Extreme Mechanics Letters*, p. 100648, 2020.

[65] J. Yang, J. S. Lee, and Y. Y. Kim, "Multiple slow waves in metaporous layers for broadband sound absorption," *Journal of Physics D: Applied Physics*, vol. 50, no. 1, p. 015301, 2016.

[66] F. J. Fahy and P. Gardonio, *Sound and structural vibration: radiation, transmission and response*. Elsevier, 2007.

[67] G. W. Milton and J. R. Willis, "On modifications of Newton's second law and linear continuum elastodynamics," in *Proceedings of the Royal Society of London A: Mathematical, Physical and Engineering Sciences*, The Royal Society, 2007.

[68] H. Huang, C. Sun, and G. Huang, "On the negative effective mass density in acoustic metamaterials," *International Journal of Engineering Science*, vol. 47, no. 4, pp. 610–617, 2009.

[69] Y. Chen, G. Huang, X. Zhou, G. Hu, and C. T. Sun, "Analytical coupled vibroacoustic modeling of membrane-type acoustic metamaterials: Membrane model," *The Journal of the Acoustical Society of America*, vol. 136, no. 3, pp. 969–979, 2014.

[70] Z. Yang, J. Mei, M. Yang, N. Chan, and P. Sheng, "Membrane-type acoustic metamaterial with negative dynamic mass," *Physical Review Letters*, vol. 101, no. 20, p. 204301, 2008.

[71] S. Yao, X. Zhou, and G. Hu, "Experimental study on negative effective mass in a 1d mass–spring system," *New Journal of Physics*, vol. 10, no. 4, p. 043020, 2008.

[72] S. Yao, X. Zhou, and G. Hu, "Investigation of the negative-mass behaviors occurring below a cut-off frequency," *New Journal of Physics*, vol. 12, no. 10, p. 103025, 2010.

[73] X. Zhou and G. Hu, "Superlensing effect of an anisotropic metamaterial slab with near-zero dynamic mass," *Applied Physics Letters*, vol. 98, no. 26, p. 263510, 2011.

[74] S. H. Lee, C. M. Park, Y. M. Seo, Z. G. Wang, and C. K. Kim, "Acoustic metamaterial with negative density," *Physics Letters A*, vol. 373, no. 48, pp. 4464–4469, 2009.

[75] C. J. Naify, C. M. Chang, G. McKnight, and S. Nutt, "Transmission loss and dynamic response of membrane-type locally resonant acoustic metamaterials," *Journal of Applied Physics*, vol. 108, no. 11, p. 114905, 2010.

[76] R. Chanaud, "Effects of geometry on the resonance frequency of helmholtz resonators," *Journal of Sound and Vibration*, vol. 178, no. 3, pp. 337–348, 1994.

[77] C. R. Liu, J. H. Wu, Z. Yang, and F. Ma, "Ultra-broadband acoustic absorption of a thin microperforated panel metamaterial with multi-order resonance," *Composite Structures*, vol. 246, p. 112366, 2020.
[78] H. Zhao, Q. Zheng, Y. Wang, J. Cao, C. Wang, and J. Wen, "Acoustic absorption of a metamaterial panel: Mechanism, boundary effect and experimental demonstration," *Applied Acoustics*, vol. 184, p. 108369, 2021.
[79] S. Ren, L. Van Belle, C. Claeys, F. X. Xin, T. J. Lu, E. Deckers, and W. Desmet, "Improvement of the sound absorption of flexible micro-perforated panels by local resonances," *Mechanical Systems and Signal Processing*, vol. 117, pp. 138–156, 2019.
[80] B. Moore, T. Jaglinski, D. Stone, and R. Lakes, "Negative incremental bulk modulus in foams," *Philosophical Magazine Letters*, vol. 86, no. 10, pp. 651–659, 2006.
[81] L. Lu, T. Yamamoto, M. Otomori, T. Yamada, K. Izui, and S. Nishiwaki, "Topology optimization of an acoustic metamaterial with negative bulk modulus using local resonance," *Finite Elements in Analysis and Design*, vol. 72, pp. 1–12, 2013.
[82] Y. Ding, Z. Liu, C. Qiu, and J. Shi, "Metamaterial with simultaneously negative bulk modulus and mass density," *Physical Review Letters*, vol. 99, no. 9, p. 093904, 2007.
[83] Y. Cheng, J. Xu, and X. Liu, "One-dimensional structured ultrasonic metamaterials with simultaneously negative dynamic density and modulus," *Physical Review B*, vol. 77, no. 4, p. 045134, 2008.
[84] Y. Wu, Y. Lai, and Z. Q. Zhang, "Elastic metamaterials with simultaneously negative effective shear modulus and mass density," *Physical Review Letters*, vol. 107, no. 10, p. 105506, 2011.
[85] X. Liu, G. Hu, G. Huang, and C. Sun, "An elastic metamaterial with simultaneously negative mass density and bulk modulus," *Applied Physics Letters*, vol. 98, no. 25, p. 251907, 2011.
[86] R. Zhu, X. Liu, G. Hu, C. Sun, and G. Huang, "Negative refraction of elastic waves at the deep-subwavelength scale in a single-phase metamaterial," *Nature Communications*, vol. 5, 2014.
[87] M. Yang, G. Ma, Z. Yang, and P. Sheng, "Coupled membranes with doubly negative mass density and bulk modulus," *Physical Review Letters*, vol. 110, no. 13, p. 134301, 2013.
[88] H. C. Zeng, C. R. Luo, H. J. Chen, S. L. Zhai, C. L. Ding, and X. P. Zhao, "Flute-model acoustic metamaterials with simultaneously negative bulk modulus and mass density," *Solid State Communications*, vol. 173, pp. 14–18, 2013.
[89] S. Zhai, H. Chen, C. Ding, and X. Zhao, "Double-negative acoustic metamaterial based on meta-molecule," *Journal of Physics D: Applied Physics*, vol. 46, no. 47, p. 475105, 2013.
[90] H. Chen, H. Zeng, C. Ding, C. Luo, and X. Zhao, "Double-negative acoustic metamaterial based on hollow steel tube meta-atom," *Journal of Applied Physics*, vol. 113, no. 10, p. 104902, 2013.
[91] D. Smith, J. Mock, A. Starr, and D. Schurig, "Gradient index metamaterials," *Physical Review E*, vol. 71, no. 3, p. 036609, 2005.
[92] S. Larouche and D. R. Smith, "Reconciliation of generalized refraction with diffraction theory," *Optics Letters*, vol. 37, no. 12, pp. 2391–2393, 2012.
[93] J. Chen, J. Xiao, D. Lisevych, A. Shakouri, and Z. Fan, "Deep-subwavelength control of acoustic waves in an ultra-compact metasurface lens," *Nature Communications*, vol. 9, no. 1, pp. 1–9, 2018.
[94] X. Jiang, B. Liang, X. Y. Zou, J. Yang, L. L. Yin, J. Yang, and J. C. Cheng, "Acoustic one-way metasurfaces: asymmetric phase modulation of sound by subwavelength layer," *Scientific Reports*, vol. 6, p. 28023, 2016.
[95] X. S. Li, Y. F. Wang, A. L. Chen, and Y. S. Wang, "Modulation of out-of-plane reflected waves by using acoustic metasurfaces with tapered corrugated holes," *Scientific Reports*, vol. 9, 2019.
[96] K. Tang, C. Qiu, M. Ke, J. Lu, Y. Ye, and Z. Liu, "Anomalous refraction of airborne sound through ultrathin metasurfaces," *Scientific Reports*, vol. 4, no. 1, pp. 1–7, 2014.
[97] Y. Xie, A. Konneker, B. I. Popa, and S. A. Cummer, "Tapered labyrinthine acoustic metamaterials for broadband impedance matching," *Applied Physics Letters*, vol. 103, no. 20, p. 201906, 2013.
[98] R. Ghaffarivardavagh, J. Nikolajczyk, R. G. Holt, S. Anderson, and X. Zhang, "Horn-like space-coiling metamaterials toward simultaneous phase and amplitude modulation," *Nature Communications*, vol. 9, no. 1, pp. 1–8, 2018.
[99] R. Al Jahdali and Y. Wu, "High transmission acoustic focusing by impedance-matched acoustic meta-surfaces," *Applied Physics Letters*, vol. 108, no. 3, p. 031902, 2016.
[100] W. Tang, C. Ren, S. Tong, and X. Huang, "Sandwich-like space-coiling metasurfaces for weak-dispersion high-efficiency transmission," *Applied Physics Letters*, vol. 115, no. 13, p. 134102, 2019.
[101] S. W. Fan, S. D. Zhao, A. L. Chen, Y. F. Wang, B. Assouar, and Y. S. Wang, "Tunable broadband reflective acoustic metasurface," *Physical Review Applied*, vol. 11, no. 4, p. 044038, 2019.
[102] S. W. Fan, S. D. Zhao, L. Cao, Y. Zhu, A. L. Chen, Y. F. Wang, K. Donda, Y. S. Wang, and B. Assouar, "Reconfigurable curved metasurface for acoustic cloaking and illusion," *Physical Review B*, vol. 101, no. 2, p. 024104, 2020.
[103] K. Donda, Y. Zhu, S.-W. Fan, L. Cao, Y. Li, and B. Assouar, "Extreme low-frequency ultrathin acoustic absorbing metasurface," *Applied Physics Letters*, vol. 115, no. 17, p. 173506, 2019.
[104] H. Chang, L. Liu, C. Zhang, and X. Hu, "Broadband high sound absorption from labyrinthine metasurfaces," *AIP Advances*, vol. 8, no. 4, p. 045115, 2018.
[105] X. Wang, D. Mao, and Y. Li, "Broadband acoustic skin cloak based on spiral metasurfaces," *Scientific Reports*, vol. 7, no. 1, pp. 1–7, 2017.
[106] K. Miyata, Y. Noguchi, T. Yamada, K. Izui, and S. Nishiwaki, "Optimum design of a multi-functional acoustic metasurface using topology optimization based on zwicker's loudness model," *Computer Methods in Applied Mechanics and Engineering*, vol. 331, pp. 116–137, 2018.
[107] C. Ding, X. Zhao, H. Chen, S. Zhai, and F. Shen, "Reflected wavefronts modulation with acoustic metasurface based on double-split hollow sphere," *Applied Physics A*, vol. 120, no. 2, pp. 487–493, 2015.
[108] X. Liu, X. Zeng, D. Gao, W. Shen, J. Wang, and S. Wang, "Experimental realization for abnormal reflection caused by an acoustic metasurface with subwavelength apertures," *Journal of Physics D: Applied Physics*, vol. 50, no. 12, p. 125303, 2017.

[109] Y. Zhu and B. Assouar, "Multifunctional acoustic metasurface based on an array of helmholtz resonators," *Physical Review B*, vol. 99, no. 17, p. 174109, 2019.
[110] J. Guo and J. Zhou, "An ultrathin acoustic carpet cloak based on resonators with extended necks," *Journal of Physics D: Applied Physics*, vol. 53, no. 50, p. 505501, 2020.
[111] Z. Chen, F. Yan, M. Negahban, and Z. Li, "Resonator-based reflective metasurface for low-frequency underwater acoustic waves," *Journal of Applied Physics*, vol. 128, no. 5, p. 055305, 2020.
[112] J. Li, A. Song, and S. A. Cummer, "Bianisotropic acoustic metasurface for surface-wave-enhanced wavefront transformation," *Physical Review Applied*, vol. 14, no. 4, p. 044012, 2020.
[113] X. Peng, J. Li, C. Shen, and S. A. Cummer, "Efficient scattering-free wavefront transformation with power flow conformal bianisotropic acoustic metasurfaces," *Applied Physics Letters*, vol. 118, no. 6, p. 061902, 2021.
[114] T. Y. Huang, C. Shen, and Y. Jing, "Membrane-and plate-type acoustic metamaterials," *The Journal of the Acoustical Society of America*, vol. 139, no. 6, pp. 3240–3250, 2016.
[115] H. Tang, Z. Chen, N. Tang, S. Li, Y. Shen, Y. Peng, X. Zhu, and J. Zang, "Hollow-out patterning ultrathin acoustic metasurfaces for multifunctionalities using soft fiber/rigid bead networks," *Advanced Functional Materials*, vol. 28, no. 36, p. 1801127, 2018.
[116] A. Abbad, N. Atalla, M. Ouisse, and O. Doutres, "Numerical and experimental investigations on the acoustic performances of membraned helmholtz resonators embedded in a porous matrix," *Journal of Sound and Vibration*, vol. 459, p. 114873, 2019.
[117] M. Lewińska, J. van Dommelen, V. Kouznetsova, and M. Geers, "Towards acoustic metafoams: the enhanced performance of a poroelastic material with local resonators," *Journal of the Mechanics and Physics of Solids*, vol. 124, pp. 189–205, 2019.
[118] S. T. Tang, J. Lau, K. Y. A. Yeung, and Z. Yang, "Multiple-frequency perfect absorption by hybrid membrane resonators," *Applied Physics Letters*, vol. 116, no. 16, p. 161902, 2020.
[119] J. Rouquerol, F. Rouquerol, P. Llewellyn, G. Maurin, and K. S. Sing, *Adsorption by powders and porous solids: principles, methodology and applications*. Academic Press, 2013.
[120] F. Fahy, "Some applications of the reciprocity principle in experimental vibroacoustics," *Acoustical Physics*, vol. 49, no. 2, pp. 217–229, 2003.
[121] M. Delany and E. Bazley, "Acoustical properties of fibrous absorbent materials," *Applied Acoustics*, vol. 3, no. 2, pp. 105–116, 1970.
[122] J. Allard and N. Atalla, *Propagation of sound in porous media: modelling sound absorbing materials*. John Wiley & Sons, 2009.
[123] J. F. Allard and Y. Champoux, "New empirical equations for sound propagation in rigid frame fibrous materials," *The Journal of the Acoustical Society of America*, vol. 91, no. 6, pp. 3346–3353, 1992.
[124] D. L. Johnson, J. Koplik, and R. Dashen, "Theory of dynamic permeability and tortuosity in fluid-saturated porous media," *Journal of Fluid Mechanics*, vol. 176, pp. 379–402, 1987.
[125] L. Xiong, B. Nennig, Y. Aurégan, and W. Bi, "Sound attenuation optimization using metaporous materials tuned on exceptional points," *The Journal of the Acoustical Society of America*, vol. 142, no. 4, pp. 2288–2297, 2017.
[126] J. Yang, J. S. Lee, and Y. Y. Kim, "Metaporous layer to overcome the thickness constraint for broadband sound absorption," *Journal of Applied Physics*, vol. 117, no. 17, p. 174903, 2015.
[127] J. P. Groby, W. Huang, A. Lardeau, and Y. Aurégan, "The use of slow waves to design simple sound absorbing materials," *Journal of Applied Physics*, vol. 117, no. 12, p. 124903, 2015.
[128] J. P. Groby, O. Dazel, A. Duclos, L. Boeckx, and L. Kelders, "Enhancing the absorption coefficient of a backed rigid frame porous layer by embedding circular periodic inclusions," *The Journal of the Acoustical Society of America*, vol. 130, no. 6, pp. 3771–3780, 2011.
[129] A. Elliott, R. Venegas, J. Groby, and O. Umnova, "Omnidirectional acoustic absorber with a porous core and a metamaterial matching layer," *Journal of Applied Physics*, vol. 115, no. 20, p. 204902, 2014.
[130] J. Yang, J. S. Lee, H. R. Lee, Y. J. Kang, and Y. Y. Kim, "Slow-wave metamaterial open panels for efficient reduction of low-frequency sound transmission," *Applied Physics Letters*, vol. 112, no. 9, p. 091901, 2018.
[131] M. D. Guild, V. M. García-Chocano, J. Sánchez Dehesa, T. P. Martin, D. C. Calvo, and G. J. Orris, "Aerogel as a soft acoustic metamaterial for airborne sound," *Physical Review Applied*, vol. 5, no. 3, p. 034012, 2016.
[132] Y. Jin, R. Kumar, O. Poncelet, O. Mondain-Monval, and T. Brunet, "Flat acoustics with soft gradient-index metasurfaces," *Nature Communications*, vol. 10, no. 1, pp. 1–6, 2019.
[133] J. P. Groby, W. Lauriks, and T. Vigran, "Total absorption peak by use of a rigid frame porous layer backed by a rigid multi-irregularities grating," *The Journal of the Acoustical Society of America*, vol. 127, no. 5, pp. 2865–2874, 2010.
[134] Y. Fang, X. Zhang, J. Zhou, J. Guo, and X. Huang, "Acoustic metaporous layer with composite structures for perfect and quasi-omnidirectional sound absorption," *Composite Structures*, vol. 223, p. 110948, 2019.
[135] Y. Fang, X. Zhang, and J. Zhou, "Experiments on reflection and transmission of acoustic porous metasurface with composite structure," *Composite Structures*, vol. 185, pp. 508–514, 2018.
[136] Y. Fang, X. Zhang, and J. Zhou, "Acoustic porous metasurface for excellent sound absorption based on wave manipulation," *Journal of Sound and Vibration*, vol. 434, pp. 273–283, 2018.
[137] A. A. Fernández-Marín, N. Jiménez, J. P. Groby, J. Sánchez-Dehesa, and V. Romero-García, "Aerogel-based metasurfaces for perfect acoustic energy absorption," *Applied Physics Letters*, vol. 115, no. 6, p. 061901, 2019.
[138] Z. Cai, S. Zhao, Z. Huang, Z. Li, M. Su, Z. Zhang, Z. Zhao, X. Hu, Y.-S. Wang, and Y. Song, "Bubble architectures for locally resonant acoustic metamaterials," *Advanced Functional Materials*, vol. 29, no. 51, p. 1906984, 2019.
[139] N. Gao, L. Tang, J. Deng, K. Lu, H. Hou, and K. Chen, "Design, fabrication and sound absorption test of composite porous metamaterial with embedding i-plates into porous polyurethane sponge," *Applied Acoustics*, vol. 175, p. 107845, 2021.
[140] M. Miniaci, A. Krushynska, A. S. Gliozzi, N. Kherraz, F. Bosia, and N. M. Pugno, "Design and fabrication of bioinspired hierarchical dissipative elastic metamaterials," *Physical Review Applied*, vol. 10, no. 2, p. 024012, 2018.

[141] F. Casadei, T. Delpero, A. Bergamini, P. Ermanni, and M. Ruzzene, "Piezoelectric resonator arrays for tunable acoustic waveguides and metamaterials," *Journal of Applied Physics*, vol. 112, no. 6, p. 064902, 2012.
[142] F. Casadei and K. Bertoldi, "Harnessing fluid-structure interactions to design self-regulating acoustic metamaterials," *Journal of Applied Physics*, vol. 115, no. 3, p. 034907, 2014.
[143] P. Wang, F. Casadei, S. Shan, J. C. Weaver, and K. Bertoldi, "Harnessing buckling to design tunable locally resonant acoustic metamaterials," *Physical Review Letters*, vol. 113, no. 1, p. 014301, 2014.
[144] Z. Tian, C. Shen, J. Li, E. Reit, Y. Gu, H. Fu, S. A. Cummer, and T. J. Huang, "Programmable acoustic metasurfaces," *Advanced Functional Materials*, vol. 29, no. 13, p. 1808489, 2019.
[145] B. Xia, N. Chen, L. Xie, Y. Qin, and D. Yu, "Temperature-controlled tunable acoustic metamaterial with active band gap and negative bulk modulus," *Applied Acoustics*, vol. 112, pp. 1–9, 2016.
[146] S. Ning, Z. Yan, D. Chu, H. Jiang, Z. Liu, and Z. Zhuang, "Ultralow-frequency tunable acoustic metamaterials through tuning gauge pressure and gas temperature," *Extreme Mechanics Letters*, p. 101218, 2021.
[147] S. Xiao, G. Ma, Y. Li, Z. Yang, and P. Sheng, "Active control of membrane-type acoustic metamaterial by electric field," *Applied Physics Letters*, vol. 106, no. 9, p. 091904, 2015.
[148] Z. Chen, W. Zhou, and C. Lim, "Tunable frequency response of topologically protected interface modes for membrane-type metamaterials via voltage control," *Journal of Sound and Vibration*, vol. 494, p. 115870, 2021.
[149] X. Chen, X. Xu, S. Ai, H. Chen, Y. Pei, and X. Zhou, "Active acoustic metamaterials with tunable effective mass density by gradient magnetic fields," *Applied Physics Letters*, vol. 105, no. 7, p. 071913, 2014.
[150] P. Liu, X. Chen, W. Xu, and Y. Pei, "Magnetically controlled multifunctional membrane acoustic metasurface," *Journal of Applied Physics*, vol. 127, no. 18, p. 185104, 2020.
[151] A. Bergamini, T. Delpero, L. D. Simoni, L. D. Lillo, M. Ruzzene, and P. Ermanni, "Phononic crystal with adaptive connectivity," *Advanced Materials*, vol. 26, no. 9, pp. 1343–1347, 2014.
[152] C. Sugino, M. Ruzzene, and A. Erturk, "Dynamics of hybrid mechanical-electromechanical locally resonant piezoelectric metastructures," in *Smart Materials, Adaptive Structures and Intelligent Systems*, American Society of Mechanical Engineers, 2017.
[153] C. Sugino, M. Ruzzene, and A. Erturk, "An analytical framework for locally resonant piezoelectric metamaterial plates," *International Journal of Solids and Structures*, vol. 182, pp. 281–294, 2020.
[154] W. Akl and A. Baz, "Analysis and experimental demonstration of an active acoustic metamaterial cell," *Journal of Applied Physics*, vol. 111, no. 4, p. 044505, 2012.
[155] W. Akl and A. Baz, "Experimental characterization of active acoustic metamaterial cell with controllable dynamic density," *Journal of Applied Physics*, vol. 112, no. 8, p. 084912, 2012.
[156] A. Allam, A. Elsabbagh, and W. Akl, "Experimental demonstration of one-dimensional active plate-type acoustic metamaterial with adaptive programmable density," *Journal of Applied Physics*, vol. 121, no. 12, p. 125106, 2017.
[157] A. Baz, "Active acoustic metamaterial with tunable effective density using a disturbance rejection controller," *Journal of Applied Physics*, vol. 125, no. 7, p. 074503, 2019.
[158] A. Allam, A. Elsabbagh, and W. Akl, "Modeling and design of two-dimensional membrane-type active acoustic metamaterials with tunable anisotropic density," *The Journal of the Acoustical Society of America*, vol. 140, no. 5, pp. 3607–3618, 2016.
[159] E. Prohofsky, "Acoustoelectric waves in piezoelectric materials," *Journal of Applied Physics*, vol. 37, no. 13, pp. 4729–4737, 1966.
[160] T. Poole and G. Nash, "Acoustoelectric current in graphene nanoribbons," *Scientific Reports*, vol. 7, no. 1, pp. 1–9, 2017.
[161] G. S. Kino, "Acoustoelectric interactions in acoustic-surface-wave devices," *Proceedings of the IEEE*, vol. 64, no. 5, pp. 724–748, 1976.
[162] C. Ravat, É. Absil, S. Holé, and J. Lewiner, "Acoustoelectric coupling for direct electrical characterization of semiconductor devices," *Journal of applied physics*, vol. 99, no. 6, p. 063712, 2006.
[163] V. J. Gokhale and M. Rais-Zadeh, "Phonon-electron interactions in piezoelectric semiconductor bulk acoustic wave resonators," *Scientific Reports*, vol. 4, no. 1, pp. 1–10, 2014.
[164] X. Peng, Y. Wen, P. Li, A. Yang, and X. Bai, "Enhanced acoustoelectric coupling in acoustic energy harvester using dual helmholtz resonators," *IEEE transactions on ultrasonics, ferroelectrics, and frequency control*, vol. 60, no. 10, pp. 2121–2128, 2013.
[165] R. Mauro and W. Wang, "Acoustoelectric interactions in piezoelectric semiconductors," *Physical Review B*, vol. 1, no. 2, p. 683, 1970.
[166] J. Q. Shen, "Strong and weak confinement of parity-time-symmetric acoustic surface wave," *Europhysics Letters*, vol. 105, no. 1, p. 17006, 2014.
[167] X. Wang, X. Luo, H. Zhao, and Z. Huang, "Acoustic perfect absorption and broadband insulation achieved by double-zero metamaterials," *Applied Physics Letters*, vol. 112, no. 2, p. 021901, 2018.
[168] Z. Hou and B. Assouar, "Tunable elastic parity-time symmetric structure based on the shunted piezoelectric materials," *Journal of Applied Physics*, vol. 123, no. 8, p. 085101, 2018.
[169] W. Akl and A. Baz, "Multicell active acoustic metamaterial with programmable effective densities," *Journal of Dynamic Systems, Measurement, and Control*, vol. 134, no. 6, 2012.
[170] W. Akl and A. Baz, "Stability analysis of active acoustic metamaterial with programmable bulk modulus," *Smart Materials and Structures*, vol. 20, no. 12, p. 125010, 2011.
[171] B. I. Popa and S. A. Cummer, "Non-reciprocal and highly nonlinear active acoustic metamaterials," *Nature Communications*, vol. 5, no. 1, pp. 1–5, 2014.
[172] H. Zhang, Y. Xiao, J. Wen, D. Yu, and X. Wen, "Ultra-thin smart acoustic metasurface for low-frequency sound insulation," *Applied Physics Letters*, vol. 108, no. 14, p. 141902, 2016.
[173] L. Ning, Y. Z. Wang, and Y. S. Wang, "Active control of elastic metamaterials consisting of symmetric double helmholtz resonator cavities," *International Journal of Mechanical Sciences*, vol. 153, pp. 287–298, 2019.
[174] B. I. Popa, L. Zigoneanu, and S. A. Cummer, "Tunable active acoustic metamaterials," *Physical Review B*, vol. 88, no. 2, p. 024303, 2013.

[175] H. Zhang, J. Wen, Y. Xiao, G. Wang, and X. Wen, "Sound transmission loss of metamaterial thin plates with periodic subwavelength arrays of shunted piezoelectric patches," *Journal of Sound and Vibration*, vol. 343, pp. 104–120, 2015.
[176] M. Danesh and A. Ghadami, "Sound transmission loss of double-wall piezoelectric plate made of functionally graded materials via third-order shear deformation theory," *Composite Structures*, vol. 219, pp. 17–30, 2019.
[177] A. Spadoni, M. Ruzzene, and K. Cunefare, "Vibration and wave propagation control of plates with periodic arrays of shunted piezoelectric patches," *Journal of Intelligent Material Systems and Structures*, vol. 20, no. 8, pp. 979–990, 2009.
[178] X. Li, Y. Chen, R. Zhu, and G. Huang, "An active meta-layer for optimal flexural wave absorption and cloaking," *Mechanical Systems and Signal Processing*, vol. 149, p. 107324, 2021.
[179] Y. Chen, G. Hu, and G. Huang, "An adaptive metamaterial beam with hybrid shunting circuits for extremely broadband control of flexural waves," *Smart Materials and Structures*, vol. 25, no. 10, p. 105036, 2016.
[180] P. Jiao, "Emerging artificial intelligence in piezoelectric and triboelectric nanogenerators," *Nano Energy*, p. 106227, 2021.
[181] P. Jiao and A. H. Alavi, "Artificial intelligence-enabled smart mechanical metamaterials: advent and future trends," *International Materials Reviews*, vol. 66, no. 6, pp. 365–393, 2021.
[182] Y. F. Tang, B. Liang, J. Yang, J. Yang, and J. C. Cheng, "Voltage-controlled membrane-type active acoustic metasurfaces with ultrathin thickness," *Applied Physics Express*, vol. 12, no. 6, p. 064501, 2019.
[183] S. Li, J. Xu, Y. Yao, and J. Tang, "Tunable reflected acoustic wave front modulated with piezoelectric metasurfaces," *Journal of Physics D: Applied Physics*, vol. 54, no. 9, p. 095102, 2020.
[184] S. Alan, A. Allam, and A. Erturk, "Programmable mode conversion and bandgap formation for surface acoustic waves using piezoelectric metamaterials," *Applied Physics Letters*, vol. 115, no. 9, p. 093502, 2019.
[185] Z. Liang, M. Willatzen, J. Li, and J. Christensen, "Tunable acoustic double negativity metamaterial," *Scientific Reports*, vol. 2, p. 859, 2012.
[186] H. Shao, H. He, G. Chen, and Y. Chen, "Two new designs of lamp-type piezoelectric metamaterials for active wave propagation control," *Chinese Journal of Physics*, 2020.
[187] A. Bacigalupo, M. L. De Bellis, and D. Misseroni, "Design of tunable acoustic metamaterials with periodic piezoelectric microstructure," *Extreme Mechanics Letters*, vol. 40, p. 100977, 2020.
[188] M. Oudich and Y. Li, "Tunable sub-wavelength acoustic energy harvesting with a metamaterial plate," *Journal of Physics D: Applied Physics*, vol. 50, no. 31, p. 315104, 2017.
[189] S. Qi, Y. Li, and B. Assouar, "Acoustic focusing and energy confinement based on multilateral metasurfaces," *Physical Review Applied*, vol. 7, no. 5, p. 054006, 2017.
[190] X. Wang, J. Xu, J. Ding, C. Zhao, and Z. Huang, "A compact and low-frequency acoustic energy harvester using layered acoustic metamaterials," *Smart Materials and Structures*, vol. 28, no. 2, p. 025035, 2019.
[191] J. Li, X. Zhou, G. Huang, and G. Hu, "Acoustic metamaterials capable of both sound insulation and energy harvesting," *Smart Materials and Structures*, vol. 25, no. 4, p. 045013, 2016.
[192] R. U. Ahmed and S. Banerjee, "Low frequency energy scavenging using sub-wave length scale acousto-elastic metamaterial," *AIP Advances*, vol. 4, no. 11, p. 117114, 2014.
[193] M. Yuan, Z. Cao, J. Luo, and R. Ohayon, "Acoustic metastructure for effective low-frequency acoustic energy harvesting," *Journal of Low Frequency Noise, Vibration and Active Control*, vol. 37, no. 4, pp. 1015–1029, 2018.
[194] X. Zhang, H. Zhang, Z. Chen, and G. Wang, "Simultaneous realization of large sound insulation and efficient energy harvesting with acoustic metamaterial," *Smart Materials and Structures*, vol. 27, no. 10, p. 105018, 2018.
[195] M. Jin, B. Liang, J. Yang, J. Yang, and J. C. Cheng, "Ultrathin planar metasurface-based acoustic energy harvester with deep subwavelength thickness and mechanical rigidity," *Scientific Reports*, vol. 9, no. 1, pp. 1–7, 2019.
[196] M. Yuan, X. Sheng, Z. Cao, Z. Pang, and G. Huang, "Joint acoustic energy harvesting and noise suppression using deep-subwavelength acoustic device," *Smart Materials and Structures*, vol. 29, no. 3, p. 035012, 2020.
[197] K. H. Sun, J. E. Kim, J. Kim, and K. Song, "Sound energy harvesting using a doubly coiled-up acoustic metamaterial cavity," *Smart Materials and Structures*, vol. 26, no. 7, p. 075011, 2017.
[198] S. Qi, M. Oudich, Y. Li, and B. Assouar, "Acoustic energy harvesting based on a planar acoustic metamaterial," *Applied Physics Letters*, vol. 108, no. 26, p. 263501, 2016.
[199] L. Y. Wu, L. W. Chen, and C. M. Liu, "Acoustic energy harvesting using resonant cavity of a sonic crystal," *Applied Physics Letters*, vol. 95, no. 1, p. 013506, 2009.
[200] K. J. Ma, T. Tan, F. R. Liu, L. C. Zhao, W. H. Liao, and W. M. Zhang, "Acoustic energy harvesting enhanced by locally resonant metamaterials," *Smart Materials and Structures*, vol. 29, no. 7, p. 075025, 2020.
[201] T. Deng, S. Zhang, and Y. Gao, "Tunability of band gaps and energy harvesting based on the point defect in a magneto-elastic acoustic metamaterial plate," *Applied Physics Express*, vol. 13, no. 1, p. 015503, 2019.
[202] S. Qi and B. Assouar, "Acoustic energy harvesting based on multilateral metasurfaces," *Applied Physics Letters*, vol. 111, no. 24, p. 243506, 2017.
[203] S. Qi and B. Assouar, "Ultrathin acoustic metasurfaces for reflective wave focusing," *Journal of Applied Physics*, vol. 123, no. 23, p. 234501, 2018.
[204] K. Yi, M. Collet, S. Chesne, and M. Monteil, "Enhancement of elastic wave energy harvesting using adaptive piezo-lens," *Mechanical Systems and Signal Processing*, vol. 93, pp. 255–266, 2017.
[205] G. S. Liu, Y. Y. Peng, M. H. Liu, X. Y. Zou, and J. C. Cheng, "Broadband acoustic energy harvesting metasurface with coupled helmholtz resonators," *Applied Physics Letters*, vol. 113, no. 15, p. 153503, 2018.
[206] P. Eghbali, D. Younesian, and S. Farhangdoust, "Enhancement of the low-frequency acoustic energy harvesting with auxetic resonators," *Applied Energy*, vol. 270, p. 115217, 2020.

[207] M. Yuan, Z. Cao, J. Luo, and Z. Pang, "Helix structure for low frequency acoustic energy harvesting," *Review of Scientific Instruments*, vol. 89, no. 5, p. 055002, 2018.
[208] M. Yuan, Z. Cao, J. Luo, and Z. Pang, "Low frequency acoustic energy harvester based on a planar helmholtz resonator," *AIP Advances*, vol. 8, no. 8, p. 085012, 2018.
[209] R. Ahmed, D. Madisetti, and S. Banerjee, "A sub-wavelength scale acoustoelastic sonic crystal for harvesting energies at very low frequencies (< 1 khz) using controlled geometric configurations," *Journal of Intelligent Material Systems and Structures*, vol. 28, no. 3, pp. 381–391, 2017.
[210] F. Mir, M. Saadatzi, R. U. Ahmed, and S. Banerjee, "Acoustoelastic metawall noise barriers for industrial application with simultaneous energy harvesting capability," *Applied Acoustics*, vol. 139, pp. 282–292, 2018.
[211] Y. Jin, B. Bonello, and Y. Pan, "Acoustic metamaterials with piezoelectric resonant structures," *Journal of Physics D: Applied Physics*, vol. 47, no. 24, p. 245301, 2014.
[212] C. Sheng Bing, W. Ji Hong, W. Gang, and W. Xi Sen, "Tunable band gaps in acoustic metamaterials with periodic arrays of resonant shunted piezos," *Chinese Physics B*, vol. 22, no. 7, p. 074301, 2013.
[213] K. Koziol, J. Vilatela, A. Moisala, M. Motta, P. Cunniff, M. Sennett, and A. Windle, "High-performance carbon nanotube fiber," *Science*, vol. 318, no. 5858, pp. 1892–1895, 2007.
[214] A. M. Mohamed, K. Yao, Y. M. Yousry, S. Chen, J. Wang, and S. Ramakrishna, "Open-cell poly (vinylidene fluoride) foams with polar phase for enhanced airborne sound absorption," *Applied Physics Letters*, vol. 113, no. 9, p. 092903, 2018.
[215] S. Velayudham, C. H. Lee, M. Xie, D. Blair, N. Bauman, Y. K. Yap, S. A. Green, and H. Liu, "Noncovalent functionalization of boron nitride nanotubes with poly (p-phenylene-ethynylene) s and polythiophene," *ACS Applied Materials & Interfaces*, vol. 2, no. 1, pp. 104–110, 2010.
[216] H. F. Xiang, S. X. Tan, X. L. Yu, Y. H. Long, X. L. Zhang, N. Zhao, and J. Xu, "Sound absorption behavior of electrospun polyacrylonitrile nanofibrous membranes," *Chinese Journal of Polymer Science*, vol. 29, no. 6, pp. 650–657, 2011.
[217] A. Rabbi, H. Bahrambeygi, K. Nasouri, A. M. Shoushtari, and M. R. Babaei, "Manufacturing of pan or pu nanofiber layers/pet nonwoven composite as highly effective sound absorbers," *Advances in Polymer Technology*, vol. 33, no. 4, 2014.
[218] K. Qamoshi and R. Rasuli, "Subwavelength structure for sound absorption from graphene oxide-doped polyvinylpyrrolidone nanofibers," *Applied Physics A*, vol. 9, no. 122, pp. 1–7, 2016.
[219] C. M. Wu and M. H. Chou, "Polymorphism, piezoelectricity and sound absorption of electrospun pvdf membranes with and without carbon nanotubes," *Composites Science and Technology*, vol. 127, pp. 127–133, 2016.
[220] Y. Li, S. Wang, Q. Peng, Z. Zhou, Z. Yang, X. He, and Y. Li, "Active control of graphene-based membrane-type acoustic metamaterials using a low voltage," *Nanoscale*, vol. 11, no. 35, pp. 16384–16392, 2019.
[221] K. Zhang, C. Ma, Q. He, S. Lin, Y. Chen, Y. Zhang, N. X. Fang, and X. Zhao, "Metagel with broadband tunable acoustic properties over air–water–solid ranges," *Advanced Functional Materials*, vol. 29, no. 38, p. 1903699, 2019.
[222] A. Ba, A. Kovalenko, C. Aristégui, O. Mondain-Monval, and T. Brunet, "Soft porous silicone rubbers with ultra-low sound speeds in acoustic metamaterials," *Scientific Reports*, vol. 7, no. 1, pp. 1–6, 2017.
[223] M. Kushwaha, B. Djafari-Rouhani, and L. Dobrzynski, "Sound isolation from cubic arrays of air bubbles in water," *Physics Letters A*, vol. 248, no. 2-4, pp. 252–256, 1998.
[224] V. Leroy, A. Bretagne, M. Fink, H. Willaime, P. Tabeling, and A. Tourin, "Design and characterization of bubble phononic crystals," *Applied Physics Letters*, vol. 95, no. 17, p. 171904, 2009.
[225] T. Brunet, A. Merlin, B. Mascaro, K. Zimny, J. Leng, O. Poncelet, C. Aristégui, and O. Mondain-Monval, "Soft 3d acoustic metamaterial with negative index," *Nature Materials*, vol. 14, no. 4, pp. 384–388, 2015.
[226] Z. Huang, M. Su, Q. Yang, Z. Li, S. Chen, Y. Li, X. Zhou, F. Li, and Y. Song, "A general patterning approach by manipulating the evolution of two-dimensional liquid foams," *Nature Communications*, vol. 8, no. 1, pp. 1–9, 2017.
[227] Z. Huang, S. Zhao, M. Su, Q. Yang, Z. Li, Z. Cai, H. Zhao, X. Hu, H. Zhou, F. Li, *et al.*, "Bioinspired patterned bubbles for broad and low-frequency acoustic blocking," *ACS Applied Materials & Interfaces*, vol. 12, no. 1, pp. 1757–1764, 2019.
[228] Y. Zhang, Z. Huang, Z. Cai, Y. Ye, Z. Li, F. Qin, J. Xiao, D. Zhang, Q. Guo, Y. Song, *et al.*, "Magnetic-actuated "capillary container" for versatile three-dimensional fluid interface manipulation," *Science Advances*, vol. 7, no. 34, p. eabi7498, 2021.
[229] D. Gritsenko and R. Paoli, "Theoretical optimization of trapped-bubble-based acoustic metamaterial performance," *Applied Sciences*, vol. 10, no. 16, p. 5720, 2020.
[230] Z. Huang, S. Zhao, Y. Zhang, Z. Cai, Z. Li, J. Xiao, M. Su, Q. Guo, C. Zhang, Y. Pan, *et al.*, "Tunable fluid-type metasurface for wide-angle and multifrequency water-air acoustic transmission," *Research*, vol. 2021, 2021.